Human mesenchymal stem cells (hMSCs) differentiate into an osteogenic lineage in presence of strontium containing bioactive glass nanoparticles

Parichart Naruphontjirakul[a,b], Olga Tsigkou[c], Siwei Li[a], Alexandra E. Porter[a], Julian R. Jones[a*]

[a] Department of Materials, Imperial College London, South Kensington Campus, London, SW7 2AZ UK

[b] now at: Biological Engineering Program, Faculty of Engineering, King Mongkut's University of Technology Thonburi, Bangkok, 10140, Thailand

[c] School of Materials, University of Manchester, Manchester, M1 3BB, UK

*julian.r.jones@imperial.ac.uk

Abstract

While bioactive glass and ions released during its dissolution are known to stimulate osteoblast cells, the effect bioactive glass has on human stem cells is not clear. Here, we show that spherical monodispersed strontium containing bioactive nanoparticles (Sr-BGNPs) of composition 90.6 mol% SiO_2, 5.0 mol% CaO, 4.4% mol% SrO (4.4%Sr-BGNPs) and 88.8 mol% SiO_2, 1.8 mol% CaO, and 9.4 mol% SrO (9.4%Sr-BGNPs) stimulate bone marrow derived human stem cell (hMSC) differentiation down an osteogenic pathway without osteogenic supplements. The particles were synthesised using a modified Stöber process and had diameters of 90 ± 10 nm. Previous work on similar particles that did not contain Sr (80 mol% SiO_2, 20 mol% CaO) showed stem cells did not differentiate when exposed to the particles. Here, both compositions of the Sr-BGNPs (up to concentration of 250 μg/mL) stimulated the early-, mid-, and late-stage markers of osteogenic differentiation and accelerated mineralisation in the absence of osteogenic supplements. Sr ions play a key role in osteogenic stem cell differentiation. Sr-BGNP dissolution products did not adversely affect hMSC viability and no significant differences in viability were measured between each particle composition. Confocal and transmission electron microscopy (TEM) demonstrated that monodispersed Sr-

BGNPs were internalised and localised within vesicles in the cytoplasm of hMSCs. Degradation of particles inside the cells was observed, whilst maintaining effective cations (Ca and Sr) in their silica network after 24 h in culture. The uptake of Sr-BGNPs by hMSCs was reduced by inhibitors of specific routes of endocytosis, indicating that the Sr-BGNPs uptake by hMSCs was probably via mixed endocytosis mechanisms. Sr-BGNPs have potential as injectable therapeutic devices for bone regeneration or treatment of conditions such as osteoporosis, because of their ability deliver a sustained release of osteogenic inorganic cations, e.g. calcium (Ca) or and strontium (Sr), through particle degradation locally to cells.

Statement of Significance

Here, we show that 90 nm spherical strontium containing bioactive nanoparticles of stimulate bone marrow derived human stem cell (hMSC) differentiation down an osteogenic pathway without the use of osteogenic supplements. While bioactive glass and its dissolution products are known to promote excellent bone regeneration in vivo and to stimulate osteoblast cells to produce bone matrix in vitro, their effect on human stem cells is not clear. Previously our nanoparticles that contained only SiO_2 and CaO did not provoke human bone marrow or adipose derived stem cell differentiation.

Introduction

Bone diseases are associated with an increased fracture risk, and are projected to increase dramatically with our aging population [1], with 40% of postmenopausal women affected by osteoporosis [2]. Osteoporosis occurs due to the imbalance of bone resorption and formation rates, resulting in a reduction of bone mass, leading to a higher incidence of severe fractures. This condition is becoming a major worldwide epidemic [3], with 1.5 million osteoporotic fractures occurring each year in the USA alone [4] and those that occur at the hip and spine can result in disability and high healthcare costs [5]. Osteoporosis can be considered a major public health and economic problem [6]. Current treatments target reduction of bone resorption by, for example, suppressing osteoclast activities, such as treatment with oestrogen, calcitonin, and bisphosphonates [7]. Bisphosphonates can strongly bind to bone mineral [8] and are retained within it [9], reducing rate of bone resorption by osteoclasts [8, 10-13]. Alendronate, risedronate and zoledronate have been demonstrated, in clinical trials of 3–5 years duration, to be effective drugs in terms of stabilising bone loss and maintain bone mineral density [10, 14]. However, recent literature reports a relationship between prolonged bisphosphonate therapy and atypical fractures of the femur [10, 13-17] and bisphosphonate treated patients had lower bone strength (even with typical fractures) caused by the accumulation of microcracks [13, 16, 17].

The oral drug strontium ranelate (SrR) was approved by the European Medicines Agency (EMA) [18] for osteoporosis treatment [19-22]. It was effective [19, 21, 23, 24] as it increased bone density by both promoting osteoblast activity and inhibiting osteoclasts [25**,** 26] *via* a calcium-sensing receptor (CaSR) [27, 28] by stimulating mRNA and protein levels of osteoprotegerin (OPG) and inhibiting those of the receptor activator of the NF-κB ligand (RANKL) [27, 29]. However, in 2013, the EMA released a report that SrR increased the risk of myocardial infarction [30-32] and so production was halted in August 2017 [24]. One reason for its negative side effect could be that the drug was administered systemically.

Bioactive glasses (BGs) have been used for orthopaedic and dental applications [33] because they form a strong bond to living bone [34, 35] and biodegrade, releasing ions locally [36, 37] to promote osteogenesis. The original 45S5 Bioglass® (46.1 mol% SiO_2, 24.4 mol% Na_2O, 26.9

mol% CaO, and 2.6 mol% P_2O_5) was made by the traditional melt-quench route [34]. Synthetic bone grafts based on the 45S5 Bioglass composition, such as NovaBone® (NovaBone Products LLC, Jacksonville, Florida), Biogran® (Biomet 3i, Palm Beach Gardens, Florida) and PerioGlas (NovaBone® Products LLC, Jacksonville, Florida) have been used in more than 1.5 million patients [33].

The osteogenic properties of Bioglass were attributed to soluble silica and calcium ions released from the original 45S5 Bioglass. The dissolution products activated the expression of osteoblast mitogenic growth factor and insulin-like growth factor II (IGF-II) in primary human osteoblasts (HOBs) *in vitro* [38]. These products enhanced the cytosolic calcium concentration inside osteoblasts and adenosine triphosphate (ATP) production [39]**.** The ions also up-regulated the gene expression (cDNA microarray profiles) related to osteoblast metabolism and bone homeostasis, e.g. a c-myc responsive growth related gene (RCL), which is a growth promoting gene in osteoblasts and metalloproteinases such as MMP-2 and MMP-14 that indicate extracellular matrix remodelling [36]. Bioactive glass sub-micron particles (BGSMPs) have been reported to stimulate differentiation of foetal osteoblasts towards the osteogenic lineage [40, 41]**,** and bioactive glass nanoparticles (BGNPs) promoted the differentiation of pre-osteoblasts [42, 43]. BGNPs can be considered as a reservoir that can locally deliver therapeutic agents [44-46].

The effect of Bioglass and its dissolution products on stem cells is less clear and there is some contradictory evidence in the literature. Osteogenic differentiation of human bone marrow stem cells (hMSCs) in contact with BGs was investigated [47-53], but results varied depending on the particular types of stem cells tested. Some articles found no effect on stem cells *in vitro*: Bioglass 45S5 did not stimulate the alkaline phosphatase (ALP) activity of hMSCs from five different human donors [54] and a Bioglass 45S5 coating on a polymeric substrate had no direct effect on osteoprogenitor cell differentiation or bone formation [55]. BGSMPs did not induce ALP activity or early markers of osteogenic differentiation of MSCs or adipose-derived stem cells (ADSCs) when cultured without osteogenic supplements, even though they were internalised inside the cells and caused no toxicity [56]. Others have shown that BGs enhance osteogenic differentiation of different types of stem cells, for example 70S30C sol–gel bioactive glass particles (70 mol% SiO_2, 30 mol% CaO; NovaThera, UK) enhanced the

proliferation and viability of *murine* embryonic stem cells (mESCs) in 3D bioreactors [57]. The differentiation of pluripotent *murine* embryonic stem cells to osteogenic cells was also stimulated, indicated by increased mineralized nodule formation, ALP activity, and osteoblast-associated gene expression (*runx2*/*cbfa-1*) when the cells were grown in a culture medium containing dissolution products from sol-gel 58S BG (60 mol% SiO_2, 36 mol% CaO, 4 mol% P_2O_5) [58]. Osteogenic differentiation of human adipose stem cells (hASCs) cultured on two compositions of bioactive glass discs, S53P4 BG (23.0 Na_2O - 20.0 CaO - 4.0 P_2O_5 - 53.0 SiO_2, wt%) and 1-06 BG (5.9 Na_2O - 12.0 K_2O - 5.3 MgO - 22.6 CaO - 4.0 P_2O_5 - 0.2 B_2O_3 - 50.0 SiO_2, wt%), was induced, as the ALP activity and the expression of osteogenic marker genes *runx2a* and *osterix* were stimulated [59, 60]. Dissolution products of a sol-gel glass with higher phosphate content (60 mol% SiO_2, 28 mol% CaO, 12 mol% P_2O_5) also provoked mineralisation and increased mRNA expression of the osteogenic differentiation markers ALP, osteopontin and osteonectin from human dental pulp stem cells (hDPSCs) [61].

Sr substitution for Ca in BGs up-regulated osteogenic differentiation marker genes in stem cells *in vitro,* such as osteocalcin (*Bglap*) and alkaline phosphatase (*Alp*) [62, 63] and promoted osteoconduction *in vivo* [64, 65]. Sr containing BGs enhanced the osteogenic response of osteoblasts [66, 67]. According to whole-genome microarray analysis of hMSCs, Sr^{2+} released from Sr-substituted melt-derived BG particles, based on the 45S5 composition, in which 10 and 100 mol% of calcium was replaced by strontium (Sr10, and Sr100, respectively), up-regulated the expression of genes associated with differentiation to osteoblasts: osteopontin (*spp1*), glycoprotein (transmembrane) *nmb*, and bone morphogenetic protein 2 (*bmp2*) or the isoprenoid pathway farnesyl-diphosphate farnesyltransferase 1 (*fdft1*) and geranylgeranyl diphosphate synthase 1 (*ggps1*) from the hMSCs, where SrBGs activated the sterol synthesis pathway and modified membrane cholesterol and the lipid rafts [52]. Sr incorporation into sub-micron BG particles (diameter ~ 500 nm) enhanced osteogenesis of mouse mesenchymal stem cells (mMSCs) [68-72] *via* the up-regulation of mRNA and protein expression involved in NFATc and Wnt/β-catenin signalling pathways [69] and suppressed osteoclastogenesis of RAW 264.7 cells [68]. The Sr and silicate ions released from the particles elicited synergistic effects between Sr and silicate ions on osteogenesis, osteoclastogenesis and angiogenesis of rat bone marrow stromal cells (rMSCs) [73].

Here, the aim was to assess whether Sr-BGNPs with the composition 90 mol% SiO_2, 10-x mol% CaO and x mol% SrO (x = 4.4% and 9.4) stimulate differentiation of hMSCs into bone cells and to assess the effect of the amount of Sr released from the Sr-BGNPs on differentiation of hMSCs. Internalization of the particles and their uptake mechanism into the cells were also investigated. The compositions of the nanoparticles were chosen from previous work, where we found that the maximum CaO incorporation into the nanoparticles at a nominal ratio of Si:Ca of 1:1.3 (excess Ca) was 7 mol% [42, 43]. Substituting 25% of the nominal CaO for SrO increased the total cation oxides to 9.4 mol% (90.6 mol% SiO_2, 5.0 mol% CaO, 4.4 mol% SrO) and increasing the substitution to 75% increased the cation oxides to 11.6 mol% (88.8 mol% SiO_2, 1.8 mol% CaO, 9.4 mol% SrO) [43].

Another aim was to discriminate between the effects of the Sr-BGNPs internalised by the cells and their dissolution products alone (nanoparticles not present) on hMSCs. Our hypothesis was that therapeutic ions are delivered by an intracellular uptake of Sr-BGNPs by hMSCs and differences in Sr content would have a strong effect on regulation of osteogenic gene expression by hMSCs.

Materials and Methods

Reagents were purchased from Sigma–Aldrich (Dorset, UK) unless stated otherwise. Monodispersed nanoparticles were synthesised using a modified Stöber process described previously [42, 43]. To 32.92 mL of ethanol (99.5%), 4.11 mL of distilled water and 0.48 mL of ammonium hydroxide were added in a 50 ml falcon centrifuge tube and placed under ultrasonication bath for 15 min. Then, 2.5 mL of tetraethyl orthosilicate (TEOS) was gently added to the mixed solution. The sol was left under ultrasonication for 6 h to allow hydrolysis and polycondensation to complete. Silica nanoparticle (Si-NPs) were produced first, before Ca and Sr were incorporated through addition of calcium nitrate tetrahydrate (99%) and strontium nitrate tetrahydrate (99%) and calcination at 680°C. The compositions of the particles, measured by ICP-OES, following lithium metaborate fusion, were: 90.6 mol% SiO_2, 5.0 mol% CaO, 4.4 mol% SrO (termed 4.4%Sr-BGNPs) and 88.8 mol% SiO_2, 1.8 mol% CaO, 9.4 mol% SrO (termed 9.4%Sr-BGNPs).

Culture of human bone marrow mesenchymal stem cells (hMSCs)

Human bone marrow-derived mesenchymal stem cells, hMSCs (ATCC® PCS-500-012™), were expanded in T-125 cell culture flasks (Corning®; Sigma-Aldrich, UK) in basal conditions: α-MEM supplemented with 10% (v/v) foetal bovine serum (FBS), 100 U/mL penicillin and 100 µg/mL streptomycin (Gibco; Thermo Fisher Scientific, UK), at 37°C, 5% CO_2 and in a fully humidified atmosphere. The cultured medium was routinely replaced twice per week. The cells were detached with trypsin ethylenediaminetetraacetic acid (EDTA) (Gibco; Thermo Fisher Scientific, UK) and sub-cultured when the cell reached 75-90% confluency. Passage 2 and 3 of the hMSCs were used for all studies at concentration of $5x10^4$ cells/mL.

Immunophenotypic characterization and differentiation potential of hMSCs

Flow cytometry was used to assess the immunophenotypic expression of hMSCs. According to the International Society of Cellular Therapy (ISCT) the minimal criteria for human MSCs are adherence to plastic and expression of cell surface markers including CD73 (SH3), CD105 (SH2) and CD166 and lack of expression of CD45, CD34, and HLA-DR surface molecules [74]. Untreated hMSCs in suspension at P2 were labelled with FITC or PE-conjugated monoclonal antibodies for CD105, CD166, CD73, CD34, CD45 and HLA-DR (all from BD Biosciences) and analyzed by FACSCalibur (BD Biosciences). Flow cytometry data were analyzed using CellQuest (BD Biosciences) analysis software.

To induce osteogenic differentiation hMSCs at a density of $5x10^4$ cells/mL were cultured in a 6-well plate in basal α-MEM and incubated at 37°C and 5% CO_2 for 24 h for initial cell attachment. Next day, the media was changed for osteogenic media, i.e. basal α-MEM supplemented with 10 nM DEX, 100 µM L-ascorbic acid-2-phosphate and 10 mM β-glycerophosphate, which served as a positive control. Media was replaced twice weekly.

Adipogenic and chondrogenic differentiation of the hMSCs at P5 was performed as previously described [75, 76]. Briefly, to induce adipogenic differentiation, cells were first grown to 100% confluency in a 24 well plate. Then cells were cultured for 14 days in DMEM (Gibco, UK) supplemented with 10% foetal bovine serum, 100 U/ml penicillin, 100 µg/ml streptomycin (Gibco, UK), 0.2 mM Indomethacin, 0.5 mM IBMX, 10^{-6} M dexamethasone (Sigma, UK) and 10 mg/ml Human Insulin. To detect fat deposition in the cells, cells were fixed with 4% paraformaldehyde for 30 minutes at room temperature and stained with oil red O and cell nuclei were stained with hematoxylin solution for 5 min.

To induce chondrogenic differentiation, $2.5x10^5$ cells were seeded in a 15 ml polypropylene tube and centrifuged at 150 g for 10 minutes to form a pelleted cellular micromass. The micromass at the bottom of the tube was incubated in 0.5 ml of differentiation medium made up of α-MEM supplemented with 3.5 g/ml glucose, 1% (v/v) ITS-plus, 2 mM L-glutamine (Invitrogen, UK), 100 µg/ml sodium pyruvate (Invitrogen), 0.2 mM ascorbic acid 2-phosphate, 10^{-7} M dexamethasone, and 10 ng/ml transforming growth factor (TGF)-β3 (R&D Systems). After 24 h media was replaced and then subsequently again every 2 days until 28 days. Finally, the micromass was fixed with 4% paraformaldehyde for 24 h at room temperature, embedded in paraffin, cut in a microtome and stained with alcian blue for 30 min and cell nuclei were stained with hematoxylin solution for 5 min at room temperature.

Cell viability

To determine any potential cytotoxicity effect of 4.4%Sr-BGNPs and 9.4%Sr-BGNPs (direct method) and their dissolution products (indirect methods) on hMSCs, monolayers of hMSCs were plated into 96-well plates (Corning, Thermoscience, UK) at a concentration of $5x10^4$ cells/mL and left to grow and attach in the basal α-MEM for 24 h. The relationship between cell viability with nanoparticle concentration was investigated using 3-[4, 5-dimethylthiazol-2-yl]-2, 5-diphenyl tetrazolium bromide (MTT) cell viability assays, which evaluated the activity of mitochondrial enzymes, in accordance to the ISO 10993 standard. In the direct method, a pulse-chase study was used, [77, 78], where hMSCs were exposed to particle

concentrations in the range of 0.01 to 1000 µg/mL for a 24 h (pulse) and the non-internalised particles were removed by washing with phosphate-buffered saline (PBS) buffer after 24 h. MTT assay was performed after 0, 1, 3 and 7 days of culture in the basal media, without adding further particles (chase). Separately, hMSCs were exposed to dissolution ion media of the Sr-BGNPs for 1, 3 and 7 days in culture (indirect method). The dissolution ions released from the NPs over 4 h period at 37 °C in α-MEM were prepared by incubating Sr-BGNPs within dialysis tubing (SnakeSkin, VWR, molecular weight cut-off 10 kDa) in α-MEM in an incubator shaker at 37°C, 120 rpm, for 4 h and then filtering the media containing the dissolution ions through a 0.2 µm syringe filter to sterilise. After the particles were removed from the media, 10% foetal bovine serum (FBS) (v/v), 100 U/mL penicillin and 100 µg/mL streptomycin were supplemented [43]. At each time interval, the culture media was removed, and cells were incubated with MTT solution (1 mg/mL in serum-free α-MEM) for 3 h. The resulting formazan derivatives were dissolved with dimethyl sulfoxide DMSO for 20 minutes and the optical density was determined spectrophotometrically at 570 nm using a microplate reader (SpectraMax M2^e, Molecular device). Cell metabolic activity was determined in three independent experiments in six replicates (n=6). Cells cultured under the basal α-MEM were used as the positive control.

After the cells were exposed to the nanoparticles, or the media containing the 4.4% Sr-BGNPs, and 9.4%Sr-BGNP's dissolution products (using a concentration of 250 µg/mL Sr-BGNPs), for 1, 2, and 3 weeks, the total DNA was measured using Hoechst 33285 using a protocol modified from a previous publication [16]. The culture media were removed and washed with PBS. The plates were then emptied by overturning them on absorbent towelling and stored at -80°C overnight. After 100 µL of molecular water was added in each well, the plates were incubated at room temperature for 2 h. These plates were frozen at -80°C and thawed until they had reached room temperature. 100 µL of Hoechst 33285 at 20 µg/mL was added in each well. The fluorescent intensity was measure using the microplate reader (SpectraMax M2^e, Molecular device).

Osteogenic effects

The hMSCs were cultured (cell density of $5x10^4$ cells/mL) in a 6-well plate and incubated at 37°C and 5% CO_2 for 24 h for initial cell attachment. As a positive control for differentiation the hMSCs were cultured in the osteogenic media. Media was replaced twice weekly.

Cells were exposed to six types of media: basal media (negative control); osteogenic media (basal media plus osteogenic supplements); basal media containing Sr-BGNPs (at two strontium contents of 4.4% Sr-BGNP 9.4% Sr-BGNP); osteogenic media containing Sr-BGNPs; media containing the dissolution products of Sr-BGNPs; basal media containing the dissolution products Sr-BGNPs obtained using a concentration of 250 μg/mL Sr-BGNPs (at two strontium contents of 4.4% Sr-BGNP 9.4% Sr-BGNP); and osteogenic supplemented media containing the Sr-BGNP dissolution products . Media was changed every three days. The Sr-BGNPs or dissolution products were therefore reintroduced to the cells at each media change.

Cell fixation was with 4% paraformaldehyde in phosphate buffered saline (PBS). Cells were stained with an alkaline phosphate (ALP) detection kit (Merck Millipore, Middlesex, UK) according to the manufacturer's instructions. Cells were also stained with 2% Alizarin Red S in PBS at pH 4.2, to investigate whether calcified tissue formed. To quantitatively analysis of calcified nodule formation, the extracted calcified mineral using DMSO was measured at 555 nm.

Osteogenic differentiation of hMSCs into osteoblasts is important in bone formation. There are several marker genes associated with bone formation and osteoblast phenotype, including a recombinant transcription factor protein: Runx-related transcription factor 2 (*runx-2*), osterix (*osr*), *alp, osc, osp*, osteonectin (*osn*) and *bone sialoprotein* [79-82]. *Runx-2* plays a key role in regulating bone formation [83-86] and down-regulates osteogenic marker genes such as *alp*, *col1a1, osc, osp*, *osr* and *bone sialoprotein* [86, 87]. Tsui *et al.* reported that up-regulation of *runx-2*, *alp*, and *col1a1* were evaluated as early-stage osteogenic markers of hMSCs [88], and these genes are associated with extracellular matrix organisation [79, 89]. Keogh *et al.* stated that mid-stage markers such as *osn* and *bone sialoprotein* genes play an important role in a crystal nucleation [90], which engage in extracellular matrix maturation [79, 80, 91]. Several groups showed that late-stage markers such as *osc*, and *osp* regulate mineralisation and maturation of cell differentiation [80, 91, 92].

Staining was performed for key osteoblastic differentiation markers: collagen type I (Col1a1), osteocalcin (OSC) and osteopontin (OSP). After fixation, cell membranes were permeabilised for 30 min and then blocked using 1% bovine serum albumin (BSA) in PBS for 5 min. For immunostaining, rabbit IgG primary antibody (Abcam, Cambridge, UK) was applied overnight at 4°C. The secondary antibody used for immunofluorescence was the goat anti-rabbit IgG H&L conjugated with Alexa Fluor 455 (Abcam, Cambridge, UK). Nuclei were stained with 4',6-Diamidino-2-Phenylindole, Dihydrochloride (DAPI, Thermo Fisher Scientific, Hemel Hempstead, UK). To stain the cytoplasm, the CytoPainter F-actin Staining Kit -Red Fluorescence (Abcam, Cambridge, UK) was used, according to the manufacturer's instructions. Samples were imaged using a LSM-510 inverted (CF5) confocal fluorescent microscope (Zeiss).

Quantitative real-time PCR

Quantitative Real-Time PCR (qRT-PCR) was used to investigate the hMSCs gene expression profile of the osteogenic differentiation markers. The hMSCs were seeded in 6-well, and 96-well plates (at the concentration 5 x 10^4 cells/mL) and incubated for 24 h. The cells cultured under the basal α-MEM, and the osteogenic α-MEM media were used as controls.

After the exposure time (1, 2, and 3 weeks), total RNA was extracted using a total RNA isolation kit (RNeasy Mini Kit, Qiagen, Manchester, UK) from different treated cells according to the manufacturer's instructions. The total RNA concentrations were measured using a nanodrop (NANODROP 2000c Spectrophotometer, Thermo Fisher Scientific, Hemel Hempstead, UK). First strand cDNA was reverse-transcribed using SuperScript® VILO™ cDNA Synthesis Kit (Thermo Fisher Scientific, Hemel Hempstead, UK) following the manufacture's protocol. Then RT-PCR was performed using QuantStudio6 (Thermo Fisher Scientific, Hemel Hempstead, UK). RT-PCR reactions were prepared using a Fast SYBR™ Green Master Mix (Thermo Fisher Scientific, Hemel Hempstead, UK) following the manufacture's protocol. The sequences of the primer pairs in this experiment are shown in Table 2. The qRT-PCR results were analysed using the QuantStudioTM Real-Time PCR software (Thermo Fisher Scientific, Hemel Hempstead, UK). Then relative gene expression of each gene was calculated by the

comparative $2^{-\Delta\Delta}$Ct method, where the target is normalized to reference gene GAPDH. All reactions were carried out in four samples.

Endocytosis

Understanding the uptake mechanism of Sr-BGNPs into cells would be beneficial to optimise use of the nanoparticles as intracellular delivery vehicles for therapeutic ions. In this section, the mechanism used by the nanoparticles inside the hMSCs was investigated under specific inhibitors, using a microplate reader and confocal fluorescent microscope (Scheme 1) and by transmission electron microscopy (TEM) (Scheme 2).

To further follow the mechanism of cellular uptake of Sr-BGNPs by hMSCs, under specific uptake inhibitors, the Sr-BGNPs were fluorescently labelled by functionalisation with 3-aminopropyltriethoxysilane (APTES) for covalent conjugation with fluorescein isothiocyanate (FITC), as described in our previous work [43]**.** To monitor the cellular uptake of the FITC-9.4%Sr-BGNPs, the hMSCs were exposed to 250 µg/mL of FITC-9.4%Sr-BGNPs in medium for 4 and 24 h. For 3D confocal microscopy imaging, the hMSCs were grown on a µ-Dish$^{35mm,\ low}$ (Ibidi, Germany) and treated with five inhibitors of endocytosis at 37°C for 2 h: 23 µM of wor (phagocytosis inhibitor); 1 mM of ami (macropinocytosis inhibitor); 4 µM of cyt D (micropinocytosis inhibitor); 37 µM of gen (clathrin-independent endocytosis inhibitor) and 30 µM of chlor (clathrin-dependent endocytosis inhibitor). Concentrations of the inhibitors were selected from previous work [93]. When the inhibitors were removed, the cells were treated with FITC-9.4%Sr-BGNPs at 250 µg/mL at 37°C for 24 h. Cells were fixed with 4% (w/v) paraformaldehyde in PBS at room temperature for 2 h and washed with PBS prior to subsequent incubation with Alexa 568-conjugated phalloidin (1:100, Molecular Probes, UK). The cells' nuclei were stained with 4',6-Diamidino-2-Phenylindole, Dihydrochloride (DAPI, Thermo Fisher Scientific, Hemel Hempstead, UK). Samples were imaged using a Zeiss LSM-510 inverted microscope.

For quantitative analysis, following exposure with FITC-9.4%Sr-BGNPs, the hMSCs were washed to remove any excess particles and were then lysed using the lysate solution

CelLytic™ M. FITC in the solution was measured (λ_{ex} 490 nm and λ_{em} 525 nm) using the microplate reader (SpectraMax M2^{e}, Molecular device).

For TEM analysis, after the hMSCs were exposed to 250 µg/mL of 9.4%Sr-BGNPs in medium for 24 h, they were then gently washed with 0.9% saline (NaCl) and fixed in 2% glutaraldehyde and 2% formaldehyde in 0.1 M sodium cacodylate buffer pH 7.4 at room temperature for 1 h. The fixative was removed, and the cells were rinsed with 0.1 M sodium cacodylate buffer to remove all unbound glutaraldehyde. The monolayer cell was scraped in 0.1 M sodium cacodylate buffer. The scraped cells were centrifuged to collect the cell pellets (13,000-15,000 rpm, 30 min) followed by incubation in a solution of 1% (w/v) osmium tetroxide containing 2 mM calcium chloride ($CaCl_2$) in 0.1 M sodium cacodylate buffer for 1 h at room temperature. The stained cells were then washed with DI water and dehydrated in a series of graded solutions of dried ethanol (50%, 70%, 95% and 100%) and dried acetonitrile, which were pre-dried using the molecular sieve 3A overnight for 5 min, twice in each solution. Samples were then infiltrated with resin (23.5 g Epon, 12.5g DDSA, 14 g NMA, and 0.75 mL BDMA), starting with 25%, 50% and 75% resin in acetonitrile (spinning for 30 s at 6,000 rpm). These samples were embedded in 100% resin at 100°C for 2 h. Thin sections (60–90 nm) were cut using a 35° diamond knife on a Leica Ultracut UCT ultra-microtome and collected immediately onto bare 300 mesh copper grids [41]. TEM imaging and energy dispersive X-ray spectroscopy (EDX) were performed with a JEOL 2100 Plus microscope, operated at 80 kV. Multiple cells from 2 cell samples were observed in the TEM.

Statistics

Statistical analyses were performed by one-way analysis of variance (ANOVA) in Minitab with the appropriate post hoc comparison test (Tukey's test). A *p-value < 0.05* was considered significant. The graphs shown present the results as the mean value with the standard deviation (SD) as the error bars.

Results and Discussion

Our previous study demonstrated that monodispersed spherical Sr-BGNPs can be synthesised, with diameters in the range of 80 – 100 nm, through a modified Stöber process and that the Sr-BGNPs provoked osteogenic behaviour of osteoblasts e.g. expression of Col1a1, OSC and OSP without causing DNA damage [42, 43]. Table 1 shows the measured compositions of the 4.4%Sr-BGNPs and 9.4%Sr-BGNPs used in our previous paper, wherein XRD showed that they were fully amorphous [43]. Pure dense silica nanoparticles (Si-NPs) were used as a control in the cell viability study.

Nanoparticle internalisation by hMSCs

When hMSCs were exposed to Sr-BGNPs, the NPs were internalised by the hMSCs (Fig. 1a-d). After 24 h of cell incubation with the Sr-BGNPs, most particles were located in large or small membrane-bound vesicles (probably lysosomes and endosomes) as indicated by the arrows in Fig. 1 (left panels). Degraded particles, indicated by their mottled appearance, low contrast on the particle surfaces and a decrease in particle size were observed inside the vesicles in the TEM (particularly in Fig. 1c), suggesting that the silicate network of Sr-BGNPs became unstable and broke down in the acidic environment of the vesicles. This result was consistent with a dissolution study on submicron bioactive glass particles (SMBGs) that had been immersed in artificial lysosomal fluid (ALF), at pH 4.5, in previous work [43]. EDX-TEM confirmed the elemental composition of the particles inside the vesicles (Fig. 1 (right panel)). The Si, Ca and Sr were detected from both degraded and un-degraded particles, indicating that Ca and Sr were released together, in a sustained manner from the Sr-BGNPs inside the cells, with some Ca and Sr remaining within the particle structure after 24 h incubation with the cells.

The uptake of NPs depends on multiple characteristics, such as surface chemistry, size and shape of particles [94-99] and on cell type [95-97, 99]**.** To confirm that FITC-9.4**%**Sr-BGNPs were internalised, the hMSCs were treated with these particles at a concentration of 250 µg/mL, without pre-treatment with inhibitors**.** Fig. 2 **and the supplementary videos** confirm that FITC-9.4**%**Sr-BGNPs were internalised within the cells and mainly located in the

cytoplasm**.** Internalization of FITC–Sr-BGNPs by MC3T3**-**E1 cells was previously reported to be mediated *via* a number of endocytosis pathways [43]. To investigate the mechanism of endocytosis in hMSCs, uptake of FITC-9.4%Sr-BGNPs in the presence of pharmacological endocytosis inhibitors was imaged and the FITC-9.4%Sr-BGNPs were still internalised by the hMSCs, after 24 h of incubation with each inhibitor (Fig. 3). Although there was a reduction in the amount of uptake of the FITC**-**9.4%Sr**-**BGNPs when the cells were treated with each of the endocytosis inhibitors, indicating that the hMSCs used endocytosis to internalise the FITC**-**9.4%Sr**-**BGNPs**.**

The total fluorescence intensity decreased when each of the endocytosis inhibitors were used, suggesting that FITC**-**9.4**%**Sr**-**BGNPs entered the hMSCs *via* a number of endocytosis pathways (Fig. 4). Under all five inhibitors, a statistically significant decrease in cellular uptake of the particles was observed ($p<0.05$), compared to cells that had not been treated with the inhibitors. However, some particles were still internalised within hMSCs that had been treated with all five inhibitors**.** There was no significant difference in the fluorescence intensity between 4 h and 24 h exposure, indicating that 4 h incubation sufficient for the hMSCs to uptake the Sr**-**BGNPs**.** Similar findings were observed for uptake of mesoporous silica nanoparticles MSNs by hMSCs [100, 101]**.** These results suggest that alternative uptake pathways may also exist**.**

Osteogenic differentiation on exposure to the nanoparticles

hMSCs cultured in the presence of the osteogenic supplements of β-glycerophosphate (β-gly), L-ascorbic acid-2-phosphate (A2P), and dexamethasone (dex) were used as the positive control for osteogenic differentiation [102, 103]. We also checked to ensure the hMSCs retained their multipotency under the chosen culture conditions at a later passage (P5) (Figure S1, supplementary information), which they did. Figure S1(a) shows that following culture of osteogenic media for 21 days, cells laid down calcified extracellular matrix indicated by positive alizarin Red S calcium deposits; following exposure to adipogenic media for 14 days Oil Red O positive lipid content in the cytoplasm was observed and after exposure to chondrogenic stimuli, they were positive for Alcian Blue (secretion of sulfated proteoglycans).

Figure S1(b) shows that the untreated hMSCs at P2 were positive for CD105, CD166 and CD73 and negative for CD34, CD45 and HLA-DR.

Having confirmed, the hMSCs remained multi-potent, we tested the hypothesis that the Sr-BGNPs and their dissolution products would induce osteogenic differentiation. The early-, mid- and late- stage osteogenic differentiation markers of hMSCs exposed to 4.4%Sr-BGNPs and 9.4%Sr-BGNPs or their dissolution products, were compared in the presence, or absence, of the osteogenic supplements. Quantitative RT-PCR was used to quantify the expression of osteogenic marker genes (the primers are listed in Table 2). The mRNA isolated from untreated hMSCs cultured under both basal and osteogenic conditions were used as the negative and positive controls, *GAPDH* was used as the house keeping gene.

In the absence of osteogenic supplements (Fig. 5), *runx-2, alp, col1a1, osn* and *bone sialoprotein* expression increased significantly ($p<0.05$) following treatment with both 4.4% Sr-BGNPs and 9.4%Sr-BGNPs and their dissolution products, compared with untreated cells, following three weeks in culture. Table 3 shows the Si, Ca and Sr concentrations in the dissolution product media. The *col1a1* expression was significantly higher in the hMSCs exposed to dissolution products of both Sr-BGNP compositions than in cells under the osteogenic condition without NPs (+++, $p<0.05$). The expression of *osn* and *bone sialoprotein* were significantly higher for hMSCs treated with both 4.4% Sr-BGNPs and 9.4%Sr-BGNPs and their dissolution ions compared to cells with no treatment in both the basal (***, $p<0.05$) and osteogenic (+++, $p<0.05$) control conditions. Signs of mineralization (*osn* and *bone sialoprotein* [104, 105]) were seen at week 2, in combination with a significant rise in *osc* and *osp* (~2 to 4.5-fold). *osr* is a zinc finger transcription factor, involved in the differentiation of hMSCs into osteoblastic cells by activating *osp* expression [106] and *osc* expression [107], meaning that *osr* is associated with late-stage osteoblast differentiation. *osr* was expressed in the groups treated with 4.4% Sr-BGNPs and 9.4%Sr-BGNPs, or their ions, significantly more after week 2 than cells cultured in both basal (**, $p<0.05$) and osteogenic (++, $p<0.05$) control conditions. The key finding here was that the Sr-BGNPs and their dissolution products have the ability to stimulate expression of the transcription factors, including *runx-2* and *osr*, and osteogenic markers, including *alp*, *col1a1*, *opn*, *osp*, *osc*, and *bone sialoprotein*, in the absence of osteogenic supplements. This implies that while soluble silica and calcium ions were

sufficient to promote enhanced osteogenesis in primary osteoblasts [36-38], strontium ions were needed in addition to silica and calcium ions for hMSC differentiation down the bone pathway.

In the presence of osteogenic supplements (Fig. 6), the osteogenic differentiation of both treated and untreated hMSCs was induced. An aim was to investigate whether the 4.4% Sr-BGNPs and 9.4%Sr-BGNPs or their dissolution ions have a synergistic effect with the osteogenic supplements on the osteogenic response of hMSCs boosting osteoblast marker gene expression. There was no significant difference between treated and untreated cells with Sr-BGNPs or their dissolution ions at the first week for all genes, except for *osp*. After two weeks however, the expression of all osteoblast marker genes was statistically significantly higher in the hMSCs treated with Sr-BGNPs and their dissolution products than for untreated cells, even when osteogenic supplements were present, after cells were cultured for week 2 (++, $p<0.05$) and week 3 (+++, $p<0.05$). Early markers of differentiation to osteoblasts (*runx-2, alp*, and *col1a1*) were higher for hMSCs treated with the Sr-BGNPs than untreated cells, indicating that Sr-BGNPs and their dissolution ions caused by the production of mineralized extracellular matrix (ECM). A significant increase in mid-stage markers (*osn*, and *bone sialoprotein*) by treated cells was observed after week 2, implying that the Sr-BGNPs and their dissolutoin ions released from the particles had positive effects on mineralization and ECM maturation. The expression of the late osteogenic differentiation markers (*osc*, *osp*, and *osr*) in treated cells was significantly enhanced when cells were exposed to Sr-BGNPs and their dissolution ions for two weeks suggesting minerailisation had occurred. Taken together, these results indicated that hMSCs treated with either Sr-BGNPs or their dissolution ions had a high capacity to differentiate into mature osteoblasts. The osteogenic responses of hMSCs were not consistent with previous work on BGNPs that only contained silica and calcium, where no ostegenic differentiation was observed [56]. A reason for these inconsistent results could be due to the the different particle compositions, and because of the heterogeneity of hMSC populations depending on the donor sources [108] of the commercial hMSCs.

Immunohistochemiscal (IHC) staining results under basal conditions also confirmed that expression of early- and late-stage osteogenic markers, including Col1a1, OSC and OSP proteins, by the hMSCs increased when hMSC cells were exposed to either the Sr-BGNPs or

their ionic dissolution products, at a concentration of 250 μg/mL, compared to the control (basal medium, Fig 7). This indicates that Sr-BGNPs and their dissolution products stimulated early- and late-stage osteogenic markers, including Col1a1, OSC and OSP in the absence of osteogenic supplements, following two weeks of culture, suggesting the formation of ECM and maturation of osteoblasts.

In the osteogenic condition, Col1a1, OSC and OSP proteins were expressed by the hMSCs, following one week of culture (Fig. 8), which might be because there is an early synergistic effect between the NPs or their dissolution products and osteogenic supplements. After two and three weeks in culture, there was no significant change between the cells treated with particles or their dissolution products and the control. These results were consistent with recent research that reported that Sr containing BGs could enhance the osteogenic differentiation of MSCs [51, 109, 110].

Alkaline phosphatase (ALP), a widely used marker of osteoblastic differentiation *in vitro* [40, 111], plays a critical role in bone matrix mineralization [92] and ALP activity is up-regulated during osteoblastic differentiation of hMSCs [102, 103]. Fig. 9 shows the expression of ALP activity (calorimetric staining) of the hMSCs treated with 4.4%Sr-BGNPs and 9.4%Sr-BGNPs, and their dissolution products, following one week (W-1), two weeks (W-2) and three weeks (W-3)**.** Considering the basal condition (Fig. 9a), incubation of cells with Sr-BGNPs and their dissolution products for one week did not significantly increase the expression of ALP compared to control (basal medium without particles); at week two, low levels of ALP were expressed when the cells were treated with Sr-BGNPs or their dissolution products; after three weeks, much more robust ALP expression in the hMSCs treated with either Sr-BGNPs or their dissolution products was observed, compared to the control. The ALP expression levels looked higher with the particles than their ions but there was no statistically significant difference between these two groups. ALP activity was not seen clearly in the basal control after 3 weeks in culture. These results suggest that the ALP stimulation resulted from the effect of particles and the ions released from the Sr-BGNPs during dissolution after 2 weeks of culture. These results were different to those reported by Tsigkou *et al.* for Sr-free bioactive glass particles, without osteogenic supplement, where the ALP activity of MSC and ADSC was not induced by the mono-SMBG [56]. These results indicated that Sr-BGNPs and their

dissolution products have the great potential to stimulate ALP expression levels of cell cultured without the osteogenic supplement which were first finding. Direct exposure to the Sr-BGNPs seemed to have more effect than dissolution products under the basal condition.

In the presence of osteogenic supplements (Fig. 9b), after one week, the effect of both Sr-BGNPs and their dissolution products on the hMSCs' ALP activity was similar to that of the control osteogenic -supplemented media without particles. After two weeks, the ALP activity was increased for all conditions, including the control, except for the OST+4.4%Sr-BGNP condition. These findings were similar to previous reports that ALP expression is present after the proliferative stage, approximately up to 2 weeks [80, 92, 112-114]. Under the osteogenic condition, more hMSCs stained positively for ALP expression.

Calcification

Alizarin Red S staining is a histochemical technique used to detect calcium deposits in tissues and cultures [115]. Mature ECM formation, which forms at the late-stage of osteogenic differentiation, was detected using Alizarin Red S staining. In the absence of osteogenic supplements (Fig. 10a), calcium formation was observed when the hMSCs were cultured with 4.4%Sr-BGNPs and 9.4%Sr-BGNPs or their dissolution products after weeks two and three, indicating more mature ECM formation by the hMSCs exposed to the Sr-BGNPs or their dissolution products compared to the control cells. In the presence of osteogenic supplements (Fig. 10b), cells exposed to Sr-BGNPs or their dissolution products also stained positively after two and three weeks in culture. The Alizarin Red S staining results also confirmed an increase in the cell growth in both basal and osteogenic conditions when the hMSCs were exposed to the Sr-BGNPs and their dissolution products.

Fig. 11 presents the quantitative analysis of calcified nodule formation by the hMSCs. Without osteogenic supplements, mature ECM formation was significantly higher when the cells were cultured with Sr-BGNPs or their dissolution products than on the blank control (basal media) (p<0.05), after weeks two and three of culture. In the osteogenic condition, the formation of mature calcified nodules in the ECM also significantly increased compared to cells cultured in the osteogenic media alone ($p < 0.05$). Due to the non-specificity of Alizarin Red S, it is

possible that false staining of Ca inside the particles may have occurred. However, hMSCs cells exposed to 9.4%Sr-BGNPs and dissolution products released from these particles showed a slightly higher level of mature ECM formation than those cells treated with 4.4%Sr-BGNPs (Fig. 11) suggesting that the amount of Ca in BGNPs did not contribute significantly to the positive staining. The results indicated that 4.4%Sr-BGNPs, 9.4%Sr-BGNPs and their dissolution products have the ability to stimulate hMSCs to form the mature ECM of bone tissue.

hMSC cell viability on exposure to nanoparticles

Cell viability (MTT, Fig. 12a) shows that the 4.4%Sr-BGNPs and 9.4%Sr-BGNPs did not cause a statistically significant reduction in the cell viability compared to the control condition at the concentration up to 250 μg/mL against the hMSCs following 7 days in culture. ISO 10993 standard states that the dissolution products of a biocompatible material should not reduce relative cell viability below 70% of those cultured in non-toxic control (cells culture on the tissue culture plate, TCP). The cell viability was similar for Sr-BGNPs between 0-250 μg/mL, but the Si-NPs started instigating an adverse effect on the hMSCs cell viability (below the 70% threshold) at the same particle concentrations. This was likely due to the highly compact silica network and slow degradation rate of dense Si-NPs [43]. The Sr-BGNPs tended to degrade more rapidly than Si-NPs and cause less toxicity [42, 43]. Cations, such as Sr disrupt the silica network, reducing the number of bridging oxygen bonds, which causes easier breakdown of the glass on contact with water [116]. The sol-gel BGNPs had lower cytotoxicity compared with the sol-gel BGMPs against MSCs [56]. The relative cell viability of particle concentrations above 500 μg/mL were all significantly reduced after seven days culture ($p<0.05$, Fig. 12(a)).

In the indirect method, after one day of culture, all of the dissolution products of 4.4%Sr-BGNPs and 9.4%Sr-BGNPs concentrations showed a significant positive effect on cell viability. The cell viability of hMSCs exposed to the dissolution products of 4.4%Sr-BGNPs and 9.4%Sr-BGNPs at 200 and 250 μg/mL significantly increased after three and seven days culture (Fig. 12(b), $p<0.05$). There was no significant decrease ($p<0.05$) in cell viability of the cells treated with ion dissolution products, indicating that they did not alter the proliferation. Similar findings were observed in our previous research in which Sr-BGNPs stimulated osteogenic differentiation of pre-osteoblasts (MC3T3-E1) [43], and Zhang *et al*. study in which Sr-

substituted sub-micron BGs (Sr-SBG) promoted proliferation of mMSCs [69]. The cell viability went up suggesting that hMSCs are becoming more metabolically active as the ion dissolution products released from Sr-BGNPs stimulated cell activities. Taken together, the cell viability results indicate that it will be possible to use Sr-BGNPs as inorganic drug carriers without reducing the cell viability at concentrations of up to 250 μg/mL. Sr-BGNP concentration at 250 μg/mL were used for the subsequent studies.

To evaluate the effect of the Sr-BGNPs on hMSC proliferation, DNA quantification was analysed measured using Hoechst 33285 to measure a total DNA (Fig. 13). Fig. 13a and (Fig. 13b) show similar trends with the relative cell number increasing as the exposure time increased in both direct and indirect culture, indicating that Sr-BGNPs or their dissolution products had no negative impact on hMSC proliferation. Interestingly, the number of hMSCs treated with particles or their dissolution products significantly increased compared to control, when cultured in both the basal condition (Fig. 13a) and the osteogenic condition (Fig. 13b) following weeks two and three of culture, respectively. These results indicated that particles and ions released from these particles could stimulate hMSC proliferation.

Compositional effects

Interestingly, no significant difference in osteogenic differentiation between 4.4% Sr-BGNPs and 9.4% Sr-BGNPs was observed. These results imply that a lower amount of Sr incorporation is better or equivalent for osteogenic marker gene expression (Figures 5 and 6), collagen and calcium production (ALP and Alizarin Red S, Figures 9-11), and metabolic cell activity (Figures 12 and 13). This would be important clinically as there are toxicity problems associated with systemic administration of Sr in the form of strontium ranelate (SrR). The low amount of Sr ion within the range of 3 – 6 ppm has potential to stimulated osteogenic responses as shown in our previous report [43]. Sr-BGNPs could be appropriate candidates as injectable therapeutic devices for bone regeneration or treatment of conditions such as osteoporosis. For osteoporosis treatment, we expect that the nanoparticles would be injected in a viscous hydrogel into areas most affected by loss of bone density [117].

Conclusions

Spherical strontium containing bioactive glass nanoparticles (Sr-BGNPs) stimulated an osteogenic response from human bone marrow MSCs (hMSCs), when cultured directly with the particles or when the cells were cultured with only the dissolved ions released from the particles, indicating that this effect was related to release of osteogenic Sr and Ca ions from the particles. This response to the particles occurred without osteogenic supplements in the media. The cell viability of the hMSCs exposed to Sr-BGNPs up to concentration 250 µg/mL was not significantly decreased. The dissolution products released from the Sr-BGNPs were not toxic to hMSCs at all concentrations tested following 7 days in culture. Sr-BGNPs and their dissolution products had the ability to stimulate stem cell proliferation and osteogenic responses in the absence of osteogenic supplements in culture. Mature ECM formation and expression of proteins associated with collagen production of hMSCs increased in the presence of both compositions of the Sr-BGNPs and their dissolution products. The expression of gene associated to early-, mid-, and late-osteogenic markers increased throughout the culture in the absence of osteogenic supplements. When osteogenic supplements were present a synergistic effect of the Sr-BGNPs and the supplements was measured. Individual Sr-BGNPs were internalised and localised in the membrane-bound vesicles within the cytoplasm of hMSCs *via* a mixed endocytosis mechanism. However, further investigations are crucial to apply such particles in medical applications including *in vivo* study. The work shows fresh evidence that low amounts of Sr incorporation induce an osteogenic response in human MSCs and the particles are non-toxic, paving the way for their future evaluation *in vivo*.

Conflicts of interest

There are no conflicts to declare.

Acknowledgements

The research work is supported by the Royal Thai Government and EPSRC (EP/M004414/1). Raw data available on request from rdm-enquiries@imperial.ac.uk.

References

[1] R.T. Burge, D. Worley, A. Johansen, S. Bhattacharyya, U. Bose, The cost of osteoporotic fractures in the UK: projections for 2000–2020, Journal of Medical Economics 4(1-4) (2001) 51-62.

[2] A. Svedbom, E. Hernlund, M. Ivergard, J. Compston, C. Cooper, J. Stenmark, E.V. McCloskey, B. Jonsson, J.A. Kanis, Osteoporosis in the European Union: a compendium of country-specific reports, Archives of osteoporosis 8 (2013) 137.

[3] J.A. Cauley, D. Chalhoub, A.M. Kassem, H. Fuleihan Gel, Geographic and ethnic disparities in osteoporotic fractures, Nature reviews. Endocrinology 10(6) (2014) 338-51.

[4] B.L. Riggs, L.J. Melton, 3rd, The worldwide problem of osteoporosis: insights afforded by epidemiology, Bone 17(5 Suppl) (1995) 505s-511s.

[5] D.G. Seeley, W.S. Browner, M.C. Nevitt, H.K. Genant, J.C. Scott, S.R. Cummings, Which fractures are associated with low appendicular bone mass in elderly women? The Study of Osteoporotic Fractures Research Group, Annals of internal medicine 115(11) (1991) 837-42.

[6] R. Burge, B. Dawson-Hughes, D.H. Solomon, J.B. Wong, A. King, A. Tosteson, Incidence and Economic Burden of Osteoporosis-Related Fractures in the United States, 2005–2025, Journal of Bone and Mineral Research 22(3) (2007) 465-475.

[7] S.G. Dahl, P. Allain, P.J. Marie, Y. Mauras, G. Boivin, P. Ammann, Y. Tsouderos, P.D. Delmas, C. Christiansen, Incorporation and distribution of strontium in bone, Bone 28(4) (2001) 446-453.

[8] R.G.G. Russell, N.B. Watts, F.H. Ebetino, M.J. Rogers, Mechanisms of action of bisphosphonates: similarities and differences and their potential influence on clinical efficacy, Osteoporosis International 19(6) (2008) 733-759.

[9] M.T. Drake, B.L. Clarke, S. Khosla, Bisphosphonates: Mechanism of Action and Role in Clinical Practice, Mayo Clinic Proceedings 83(9) (2008) 1032-1045.

[10] S. Ma, E.L. Goh, A. Jin, R. Bhattacharya, O.R. Boughton, B. Patel, A. Karunaratne, N.T. Vo, R. Atwood, J.P. Cobb, U. Hansen, R.L. Abel, Long-term effects of bisphosphonate therapy: perforations, microcracks and mechanical properties, Scientific Reports 7 (2017) 43399.

[11] F.P. Coxon, K. Thompson, M.J. Rogers, Recent advances in understanding the mechanism of action of bisphosphonates, Current Opinion in Pharmacology 6(3) (2006) 307-312.

[12] G. Boivin, P.J. Meunier, Effects of bisphosphonates on matrix mineralization, Journal of musculoskeletal & neuronal interactions 2(6) (2002) 538-43.

[13] A. Jin, J. Cobb, U. Hansen, R. Bhattacharya, C. Reinhard, N. Vo, R. Atwood, J. Li, A. Karunaratne, C. Wiles, R. Abel, The effect of long-term bisphosphonate therapy on trabecular bone strength and microcrack density, Bone & Joint Research 6(10) (2017) 602-609.

[14] B.A. Lenart, A.S. Neviaser, S. Lyman, C.C. Chang, F. Edobor-Osula, B. Steele, M.C.H. van der Meulen, D.G. Lorich, J.M. Lane, Association of low-energy femoral fractures with prolonged bisphosphonate use: a case control study, Osteoporosis international : a journal established as result of cooperation between the European Foundation for Osteoporosis and the National Osteoporosis Foundation of the USA 20(8) (2009) 1353-1362.

[15] B.A. Lenart, D.G. Lorich, J.M. Lane, Atypical Fractures of the Femoral Diaphysis in Postmenopausal Women Taking Alendronate, New England Journal of Medicine 358(12) (2008) 1304-1306.

[16] N. Kharwadkar, B. Mayne, J.E. Lawrence, V. Khanduja, Bisphosphonates and atypical subtrochanteric fractures of the femur, Bone & Joint Research 6(3) (2017) 144-153.

[17] A.A. Lloyd, B. Gludovatz, C. Riedel, E.A. Luengo, R. Saiyed, E. Marty, D.G. Lorich, J.M. Lane, R.O. Ritchie, B. Busse, E. Donnelly, Atypical fracture with long-term bisphosphonate therapy is associated with altered cortical composition and reduced fracture resistance, Proceedings of the National Academy of Sciences 114(33) (2017) 8722-8727.

[18] S. Das, J.C. Crockett, Osteoporosis – a current view of pharmacological prevention and treatment, Drug Design, Development and Therapy 7 (2013) 435-448.

[19] R. Cesareo, C. Napolitano, M. Iozzino, Strontium ranelate in postmenopausal osteoporosis treatment: a critical appraisal, International Journal of Women's Health 2 (2010) 1-6.

[20] M. Pilmane, K. Salma-Ancane, D. Loca, J. Locs, L. Berzina-Cimdina, Strontium and strontium ranelate: Historical review of some of their functions, Materials science & engineering. C, Materials for biological applications 78 (2017) 1222-1230.

[21] J.-Y. Reginster, J.-M. Kaufman, S. Goemaere, J.P. Devogelaer, C.L. Benhamou, D. Felsenberg, M. Diaz-Curiel, M.-L. Brandi, J. Badurski, J. Wark, A. Balogh, O. Bruyère, C. Roux, Maintenance of antifracture efficacy over 10 years with strontium ranelate in postmenopausal osteoporosis, Osteoporosis International 23(3) (2012) 1115-1122.

[22] J.Y. Reginster, Strontium ranelate in osteoporosis, Current pharmaceutical design 8(21) (2002) 1907-16.

[23] S. O'Donnell, A. Cranney, G.A. Wells, J. Adachi, J.-Y. Reginster, Strontium ranelate for preventing and treating postmenopausal osteoporosis, Cochrane Database of Systematic Reviews 3(4) (2006) CD005326.

[24] M.J. Bolland, A. Grey, Ten years too long: strontium ranelate, cardiac events, and the European Medicines Agency, British Medical Journal 354 (2016) 1-8.

[25] P.J. Marie, Strontium ranelate in osteoporosis and beyond: identifying molecular targets in bone cell biology, Molecular interventions 10(5) (2010) 305-12.

[26] E. Bonnelye, A. Chabadel, F. Saltel, P. Jurdic, Dual effect of strontium ranelate: Stimulation of osteoblast differentiation and inhibition of osteoclast formation and resorption in vitro, Bone 42(1) (2008) 129-138.

[27] T.C. Brennan, M.S. Rybchyn, W. Green, S. Atwa, A.D. Conigrave, R.S. Mason, Osteoblasts play key roles in the mechanisms of action of strontium ranelate, British Journal of Pharmacology 157(7) (2009) 1291-1300.

[28] J. Coulombe, H. Faure, B. Robin, M. Ruat, In vitro effects of strontium ranelate on the extracellular calcium-sensing receptor, Biochemical and Biophysical Research Communications 323(4) (2004) 1184-1190.

[29] A.S. Hurtel-Lemaire, R. Mentaverri, A. Caudrillier, F. Cournarie, A. Wattel, S. Kamel, E.F. Terwilliger, E.M. Brown, M. Brazier, The calcium-sensing receptor is involved in strontium ranelate-induced osteoclast apoptosis. New insights into the associated signaling pathways, The Journal of biological chemistry 284(1) (2009) 575-84.

[30] M.J. Bolland, A. Grey, A comparison of adverse event and fracture efficacy data for strontium ranelate in regulatory documents and the publication record, British Medical Journal open 4(10) (2014) 1-8.

[31] C. Cooper, K.M. Fox, J.S. Borer, Ischaemic cardiac events and use of strontium ranelate in postmenopausal osteoporosis: a nested case-control study in the CPRD, Osteoporos Int 25(2) (2014) 737-45.

[32] B. Abrahamsen, E.L. Grove, P. Vestergaard, Nationwide registry-based analysis of cardiovascular risk factors and adverse outcomes in patients treated with strontium ranelate, Osteoporosis International 25(2) (2014) 757-762.

[33] J.R. Jones, D.S. Brauer, L. Hupa, D.C. Greenspan, Bioglass and Bioactive Glasses and Their Impact on Healthcare, International Journal of Applied Glass Science 7(4) (2016) 423-434.

[34] L.L. Hench, R.J. Splinter, W.C. Allen, T.K. Greenlee, Bonding mechanisms at the interface of ceramic prosthetic materials, Journal of Biomedical Materials Research 5(6) (1971) 117-141.

[35] L. L. Hench, Opening Paper 2015-Some Comments on Bioglass: Four Eras of Discovery and Development, Biomedical Glasses 1 (2015) 1-11.

[36] I.D. Xynos, A.J. Edgar, L.D. Buttery, L.L. Hench, J.M. Polak, Gene-expression profiling of human osteoblasts following treatment with the ionic products of Bioglass 45S5 dissolution, Journal of biomedical materials research 55(2) (2001) 151-7.

[37] L.L. Hench, I. Xynos, A. Edgar, L. Buttery, J.M. Polak, J.P. Zhong, X.Y. Liu, J. Chang, Gene activating glasses, J Inorg Mater 17(5) (2002) 897-909.

[38] I.D. Xynos, A.J. Edgar, L.D. Buttery, L.L. Hench, J.M. Polak, Ionic products of bioactive glass dissolution increase proliferation of human osteoblasts and induce insulin-like growth factor II mRNA expression and protein synthesis, Biochem Biophys Res Commun 276(2) (2000) 461-5.

[39] I.A. Silver, J. Deas, M. Erecinska, Interactions of bioactive glasses with osteoblasts in vitro: effects of 45S5 Bioglass, and 58S and 77S bioactive glasses on metabolism, intracellular ion concentrations and cell viability, Biomaterials 22(2) (2001) 175-85.

[40] O. Tsigkou, J.R. Jones, J.M. Polak, M.M. Stevens, Differentiation of fetal osteoblasts and formation of mineralized bone nodules by 45S5 Bioglass® conditioned medium in the absence of osteogenic supplements, Biomaterials 30(21) (2009) 3542-3550.

[41] S. Labbaf, O. Tsigkou, K.H. Müller, M.M. Stevens, A.E. Porter, J.R. Jones, Spherical bioactive glass particles and their interaction with human mesenchymal stem cells in vitro, Biomaterials 32(4) (2011) 1010-1018.

[42] P. Naruphontjirakul, S.L. Greasley, S. Chen, A.E. Porter, J.R. Jones, Monodispersed strontium containing bioactive glass nanoparticles and MC3T3-E1 cellular response, Biomedical Glasses 2(1) (2016) 72–81.

[43] P. Naruphontjirakul, A.E. Porter, J.R. Jones, In vitro osteogenesis by intracellular uptake of strontium containing bioactive glass nanoparticles, Acta Biomaterialia 66 (2018) 67-80.

[44] Y. Xue, Y. Du, J. Yan, Z. Liu, P.X. Ma, X. Chen, B. Lei, Monodisperse photoluminescent and highly biocompatible bioactive glass nanoparticles for controlled drug delivery and cell imaging, Journal of Materials Chemistry B 3(18) (2015) 3831-3839.

[45] C. Vichery, J.-M. Nedelec, Bioactive Glass Nanoparticles: From Synthesis to Materials Design for Biomedical Applications, Materials 9(4) (2016) 288.

[46] M. Yu, Y. Xue, P.X. Ma, C. Mao, B. Lei, Intrinsic Ultrahigh Drug/miRNA Loading Capacity of Biodegradable Bioactive Glass Nanoparticles toward Highly Efficient Pharmaceutical Delivery, ACS Applied Materials & Interfaces 9(10) (2017) 8460-8470.

[47] M. Amaral, M.A. Costa, M.A. Lopes, R.F. Silva, J.D. Santos, M.H. Fernandes, Si3N4-bioglass composites stimulate the proliferation of MG63 osteoblast-like cells and support

the osteogenic differentiation of human bone marrow cells, Biomaterials 23(24) (2002) 4897-4906.

[48] G. Gao, A.F. Schilling, T. Yonezawa, J. Wang, G. Dai, X. Cui, Bioactive nanoparticles stimulate bone tissue formation in bioprinted three-dimensional scaffold and human mesenchymal stem cells, Biotechnology Journal 9(10) (2014) 1304-1311.

[49] M. Shamsi, M. Karimi, M. Ghollasi, N. Nezafati, M. Shahrousvand, M. Kamali, A. Salimi, In vitro proliferation and differentiation of human bone marrow mesenchymal stem cells into osteoblasts on nanocomposite scaffolds based on bioactive glass (64SiO2-31CaO-5P2O5)-poly-l-lactic acid nanofibers fabricated by electrospinning method, Materials Science and Engineering: C 78(Supplement C) (2017) 114-123.

[50] S. Kargozar, M. Mozafari, S.J. Hashemian, P. Brouki Milan, S. Hamzehlou, M. Soleimani, M.T. Joghataei, M. Gholipourmalekabadi, A. Korourian, K. Mousavizadeh, A.M. Seifalian, Osteogenic potential of stem cells-seeded bioactive nanocomposite scaffolds: A comparative study between human mesenchymal stem cells derived from bone, umbilical cord Wharton's jelly, and adipose tissue, Journal of Biomedical Materials Research Part B: Applied Biomaterials 106(1) (2018) 61-72.

[51] M. Stefanic, M. Peroglio, A.M. Stanciuc, G.C. Machado, I. Campbell, M.M. Kržmanc, M. Alini, X. Zhang, The influence of strontium release rate from bioactive phosphate glasses on osteogenic differentiation of human mesenchymal stem cells, Journal of the European Ceramic Society 38(3) (2018) 887-897.

[52] H. Autefage, E. Gentleman, E. Littmann, M.A. Hedegaard, T. Von Erlach, M. O'Donnell, F.R. Burden, D.A. Winkler, M.M. Stevens, Sparse feature selection methods identify unexpected global cellular response to strontium-containing materials, 112(14) (2015) 4280-5.

[53] M. Bosetti, M. Cannas, The effect of bioactive glasses on bone marrow stromal cells differentiation, Biomaterials 26(18) (2005) 3873-3879.

[54] G.C. Reilly, S. Radin, A.T. Chen, P. Ducheyne, Differential alkaline phosphatase responses of rat and human bone marrow derived mesenchymal stem cells to 45S5 bioactive glass, Biomaterials 28(28) (2007) 4091-4097.

[55] J. Kent Leach, D. Kaigler, Z. Wang, P.H. Krebsbach, D.J. Mooney, Coating of VEGF-releasing scaffolds with bioactive glass for angiogenesis and bone regeneration, Biomaterials 27(17) (2006) 3249-3255.

[56] O. Tsigkou, S. Labbaf, M.M. Stevens, A.E. Porter, J.R. Jones, Monodispersed Bioactive Glass Submicron Particles and Their Effect on Bone Marrow and Adipose Tissue-Derived Stem Cells, Advanced Healthcare Materials 3(1) (2014) 115-125.

[57] J. Zhang, M. Wang, J.M. Cha, A. Mantalaris, The incorporation of 70s bioactive glass to the osteogenic differentiation of murine embryonic stem cells in 3D bioreactors, Journal of Tissue Engineering and Regenerative Medicine 3(1) (2009) 63-71.

[58] R.C. Bielby, R.S. Pryce, L.L. Hench, J.M. Polak, Enhanced derivation of osteogenic cells from murine embryonic stem cells after treatment with ionic dissolution products of 58S bioactive sol-gel glass, Tissue engineering 11(3-4) (2005) 479-88.

[59] M. Ojansivu, S. Vanhatupa, L. Björkvik, H. Häkkänen, M. Kellomäki, R. Autio, J.A. Ihalainen, L. Hupa, S. Miettinen, Bioactive glass ions as strong enhancers of osteogenic differentiation in human adipose stem cells, Acta Biomaterialia 21 (2015) 190-203.

[60] M. Ojansivu, L. Hyväri, M. Kellomäki, L. Hupa, S. Vanhatupa, S. Miettinen, Bioactive glass induced osteogenic differentiation of human adipose stem cells is dependent on cell attachment mechanism and mitogen-activated protein kinases, Eur Cell Mater, 2018, pp. 54-72.

[61] A.B. Houreh, S. Labbaf, H.-K. Ting, F. Ejeian, J.R. Jones, M.-H.N. Esfahani, Influence of calcium and phosphorus release from bioactive glasses on viability and differentiation of dental pulp stem cells, Journal of Materials Science 52(15) (2017) 8928-8941.

[62] M.E. Santocildes-Romero, A. Crawford, P.V. Hatton, R.L. Goodchild, I.M. Reaney, C.A. Miller, The osteogenic response of mesenchymal stromal cells to strontium-substituted bioactive glasses, Journal of Tissue Engineering and Regenerative Medicine 9(5) (2015) 619-631.

[63] F. Yang, D.Z. Yang, J. Tu, Q.X. Zheng, L.T. Cai, L.P. Wang, Strontium Enhances Osteogenic Differentiation of Mesenchymal Stem Cells and In Vivo Bone Formation by Activating Wnt/Catenin Signaling, Stem Cells 29(6) (2011) 981-991.

[64] A. Gorustovich Alejandro, T. Steimetz, L. Cabrini Rómulo, M. Porto López José, Osteoconductivity of strontium-doped bioactive glass particles: A histomorphometric study in rats, Journal of Biomedical Materials Research Part A 92A(1) (2009) 232-237.

[65] S. Zhao, J. Zhang, M. Zhu, Y. Zhang, Z. Liu, C. Tao, Y. Zhu, C. Zhang, Three-dimensional printed strontium-containing mesoporous bioactive glass scaffolds for repairing rat critical-sized calvarial defects, Acta Biomaterialia 12 (2015) 270-280.

[66] E. Gentleman, Y.C. Fredholm, G. Jell, N. Lotfibakhshaiesh, M.D. O'Donnell, R.G. Hill, M.M. Stevens, The effects of strontium-substituted bioactive glasses on osteoblasts and osteoclasts in vitro, Biomaterials 31(14) (2010) 3949-3956.

[67] J. Isaac, J. Nohra, J. Lao, E. Jallot, J.M. Nedelec, A. Berdal, J.M. Sautier, Effects of strontium-doped bioactive glass on the differentiation of cultured osteogenic cells, Eur. Cells Mater. 21 (2011) 130-143.

[68] W. Zhang, F. Zhao, D. Huang, X. Fu, X. Li, X. Chen, Strontium-Substituted Submicrometer Bioactive Glasses Modulate Macrophage Responses for Improved Bone Regeneration, ACS Applied Materials & Interfaces 8(45) (2016) 30747-30758.

[69] W. Zhang, D. Huang, F. Zhao, W. Gao, L. Sun, X. Li, X. Chen, Synergistic effect of strontium and silicon in strontium-substituted sub-micron bioactive glass for enhanced osteogenesis, Materials Science and Engineering: C 89 (2018) 245-255.

[70] W. Zhang, F.J. Zhao, D.Q. Huang, X.L. Fu, X. Li, X.F. Chen, Strontium-Substituted Submicrometer Bioactive Glasses Modulate Macrophage Responses for Improved Bone Regeneration, ACS Appl. Mater. Interf. 8(45) (2016) 30747-30758.

[71] W. Zhang, D.Q. Huang, F.J. Zhao, W.D. Gao, L.Y. Sun, X. Li, X.F. Chen, Synergistic effect of strontium and silicon in strontium-substituted sub-micron bioactive glass for enhanced osteogenesis, Mater. Sci. Eng., C 89 (2018) 245-255.

[72] L.X. Mao, L.G. Xia, J. Chang, J.Q. Liu, L.Y. Jiang, C.T. Wu, B. Fang, The synergistic effects of Sr and Si bioactive ions on osteogenesis, osteoclastogenesis and angiogenesis for osteoporotic bone regeneration, Acta Biomater 61 (2017) 217-232.

[73] L. Mao, L. Xia, J. Chang, J. Liu, L. Jiang, C. Wu, B. Fang, The synergistic effects of Sr and Si bioactive ions on osteogenesis, osteoclastogenesis and angiogenesis for osteoporotic bone regeneration, Acta Biomaterialia 61 (2017) 217-232.

[74] M. Dominici, K. Le Blanc, I. Mueller, I. Slaper-Cortenbach, F.C. Marini, D.S. Krause, R.J. Deans, A. Keating, D.J. Prockop, E.M. Horwitz, Minimal criteria for defining multipotent mesenchymal stromal cells. The International Society for Cellular Therapy position statement, Cytotherapy 8(4) (2006) 315-317.

[75] K. Sudo, M. Kanno, K. Miharada, S. Ogawa, T. Hiroyama, K. Saijo, Y. Nakamura, Mesenchymal progenitors able to differentiate into osteogenic, chondrogenic, and/or adipogenic cells in vitro are present in most primary fibroblast-like cell populations, Stem Cells 25(7) (2007) 1610-1617.

[76] M.F. Pittenger, A.M. Mackay, S.C. Beck, R.K. Jaiswal, R. Douglas, J.D. Mosca, M.A. Moorman, D.W. Simonetti, S. Craig, D.R. Marshak, Multilineage potential of adult human mesenchymal stem cells, Science 284(5411) (1999) 143-147.

[77] M. Navas-Moreno, M. Mehrpouyan, T. Chernenko, D. Candas, M. Fan, J.J. Li, M. Yan, J.W. Chan, Nanoparticles for live cell microscopy: A surface-enhanced Raman scattering perspective, Scientific Reports 7(1) (2017) 4471.

[78] X.A. Wu, C.H.J. Choi, C. Zhang, L. Hao, C.A. Mirkin, Intracellular fate of spherical nucleic acid nanoparticle conjugates, Journal of the American Chemical Society 136(21) (2014) 7726-7733.

[79] N.A. Twine, L. Chen, C.N. Pang, M.R. Wilkins, M. Kassem, Identification of differentiation-stage specific markers that define the ex vivo osteoblastic phenotype, Bone 67 (2014) 23-32.

[80] B. Setzer, M. Bächle, M.C. Metzger, R.J. Kohal, The gene-expression and phenotypic response of hFOB 1.19 osteoblasts to surface-modified titanium and zirconia, Biomaterials 30(6) (2009) 979-990.

[81] S. Tanabe, Y. Sato, T. Suzuki, K. Suzuki, T. Nagao, T. Yamaguchi, Gene Expression Profiling of Human Mesenchymal Stem Cells for Identification of Novel Markers in Early- and Late-Stage Cell Culture, Journal of Biochemistry 144(3) (2008) 399-408.

[82] L.T.H. Nguyen, S. Liao, S. Ramakrishna, C.K. Chan, The role of nanofibrous structure in osteogenic differentiation of human mesenchymal stem cells with serial passage, Nanomedicine (London, England) 6(6) (2011) 961.

[83] J. Pratap, A. Javed, L.R. Languino, A.J. van Wijnen, J.L. Stein, G.S. Stein, J.B. Lian, The Runx2 osteogenic transcription factor regulates matrix metalloproteinase 9 in bone metastatic cancer cells and controls cell invasion, Molecular and cellular biology 25(19) (2005) 8581-91.

[84] L. Gilbert, X. He, P. Farmer, J. Rubin, H. Drissi, A.J. van Wijnen, J.B. Lian, G.S. Stein, M.S. Nanes, Expression of the osteoblast differentiation factor RUNX2 (Cbfa1/AML3/Pebp2alpha A) is inhibited by tumor necrosis factor-alpha, The Journal of biological chemistry 277(4) (2002) 2695-701.

[85] C. Shui, T.C. Spelsberg, B.L. Riggs, S. Khosla, Changes in Runx2/Cbfa1 expression and activity during osteoblastic differentiation of human bone marrow stromal cells, Journal of bone and mineral research : the official journal of the American Society for Bone and Mineral Research 18(2) (2003) 213-21.

[86] G. Karsenty, Minireview: Transcriptional Control of Osteoblast Differentiation, Endocrinology 142(7) (2001) 2731-2733.

[87] L. Thiagarajan, H.A.D.M. Abu-Awwad, J.E. Dixon, Osteogenic Programming of Human Mesenchymal Stem Cells with Highly Efficient Intracellular Delivery of RUNX2, Stem Cells Translational Medicine 6(12) (2017) 2146-2159.

[88] M.-T. Tsai, W.-J. Li, R.S. Tuan, W.H. Chang, Modulation of Osteogenesis in Human Mesenchymal Stem Cells by Specific Pulsed Electromagnetic Field Stimulation, Journal of orthopaedic research : official publication of the Orthopaedic Research Society 27(9) (2009) 1169-1174.

[89] J.B. Lian, G.S. Stein, Development of the osteoblast phenotype: molecular mechanisms mediating osteoblast growth and differentiation, The Iowa orthopaedic journal 15 (1995) 118.

[90] M.B. Keogh, F.J. O' Brien, J.S. Daly, A novel collagen scaffold supports human osteogenesis—applications for bone tissue engineering, Cell and Tissue Research 340(1) (2010) 169-177.

[91] M.-H. Choi, W.-C. Noh, J.-W. Park, J.-M. Lee, J.-Y. Suh, Gene expression pattern during osteogenic differentiation of human periodontal ligament cells in vitro, Journal of periodontal & implant science 41(4) (2011) 167-175.

[92] P. Ni, S. Fu, M. Fan, G. Guo, S. Shi, J. Peng, F. Luo, Z. Qian, Preparation of poly(ethylene glycol)/polylactide hybrid fibrous scaffolds for bone tissue engineering, International Journal of Nanomedicine 6 (2011) 3065-3075.

[93] J. Linares, M.C. Matesanz, M. Vila, M.J. Feito, G. Gonçalves, M. Vallet-Regí, P.A.A.P. Marques, M.T. Portolés, Endocytic Mechanisms of Graphene Oxide Nanosheets in Osteoblasts, Hepatocytes and Macrophages, ACS Appl. Mater. Interf. 6(16) (2014) 13697-13706.

[94] A. Albanese, P.S. Tang, W.C. Chan, The effect of nanoparticle size, shape, and surface chemistry on biological systems, Annual review of biomedical engineering 14 (2012) 1-16.

[95] M.H. Kafshgari, F.J. Harding, N.H. Voelcker, Insights into cellular uptake of nanoparticles, Current drug delivery 12(1) (2015) 63-77.

[96] I.M. Adjei, B. Sharma, V. Labhasetwar, Nanoparticles: Cellular Uptake and Cytotoxicity, in: D.G. Capco, Y. Chen (Eds.), Nanomaterial: Impacts on Cell Biology and Medicine, Springer Netherlands, Dordrecht, 2014, pp. 73-91.

[97] N. Oh, J.-H. Park, Endocytosis and exocytosis of nanoparticles in mammalian cells, International Journal of Nanomedicine 9(Suppl 1) (2014) 51-63.

[98] Q. Gan, D. Dai, Y. Yuan, J. Qian, S. Sha, J. Shi, C. Liu, Effect of size on the cellular endocytosis and controlled release of mesoporous silica nanoparticles for intracellular delivery, Biomedical Microdevices 14(2) (2012) 259-270.

[99] S.-H. Wu, Y. Hung, C.-Y. Mou, Mesoporous silica nanoparticles as nanocarriers, Chemical Communications 47(36) (2011) 9972-9985.

[100] D.M. Huang, Y. Hung, B.S. Ko, S.C. Hsu, W.H. Chen, C.L. Chien, C.P. Tsai, C.T. Kuo, J.C. Kang, C.S. Yang, C.Y. Mou, Y.C. Chen, Highly efficient cellular labeling of mesoporous nanoparticles in human mesenchymal stem cells: implication for stem cell tracking, FASEB

journal : official publication of the Federation of American Societies for Experimental Biology 19(14) (2005) 2014-6.

[101] T.-H. Chung, S.-H. Wu, M. Yao, C.-W. Lu, Y.-S. Lin, Y. Hung, C.-Y. Mou, Y.-C. Chen, D.-M. Huang, The effect of surface charge on the uptake and biological function of mesoporous silica nanoparticles in 3T3-L1 cells and human mesenchymal stem cells, Biomaterials 28(19) (2007) 2959-2966.

[102] F.P. Barry, J.M. Murphy, Mesenchymal stem cells: clinical applications and biological characterization, The International Journal of Biochemistry & Cell Biology 36(4) (2004) 568-584.

[103] M.J. Coelho, M.H. Fernandes, Human bone cell cultures in biocompatibility testing. Part II: effect of ascorbic acid, β-glycerophosphate and dexamethasone on osteoblastic differentiation, Biomaterials 21(11) (2000) 1095-1102.

[104] B. Ganss, R.H. Kim, J. Sodek, Bone Sialoprotein, Critical Reviews in Oral Biology & Medicine 10(1) (1999) 79-98.

[105] P. Tambasco de Oliveira, A. Nanci, Nanotexturing of titanium-based surfaces upregulates expression of bone sialoprotein and osteopontin by cultured osteogenic cells, Biomaterials 25(3) (2004) 403-413.

[106] Y.-J. Kim, H.-N. Kim, E.-K. Park, B.-H. Lee, H.-M. Ryoo, S.-Y. Kim, I.-S. Kim, J.L. Stein, J.B. Lian, G.S. Stein, A.J. van Wijnen, J.-Y. Choi, The bone-related Zn finger transcription factor Osterix promotes proliferation of mesenchymal cells, Gene 366(1) (2006) 145-151.

[107] K. Nakashima, X. Zhou, G. Kunkel, Z. Zhang, J.M. Deng, R.R. Behringer, B. de Crombrugghe, The Novel Zinc Finger-Containing Transcription Factor Osterix Is Required for Osteoblast Differentiation and Bone Formation, Cell 108(1) (2002) 17-29.

[108] S. Sundelacruz, M. Levin, D.L. Kaplan, Comparison of the depolarization response of human mesenchymal stem cells from different donors, Scientific Reports 5 (2015) 18279.

[109] F. Yang, D. Yang, J. Tu, Q. Zheng, L. Cai, L. Wang, Strontium Enhances Osteogenic Differentiation of Mesenchymal Stem Cells and In Vivo Bone Formation by Activating Wnt/Catenin Signaling, Stem Cells 29(6) (2011) 981-991.

[110] J. Isaac, J. Nohra, J. Lao, E. Jallot, J.-M. Nedelec, A. Berdal, J.-M. Sautier, Effects of strontium-doped bioactive glass on the differentiation of cultured osteogenic cells, Eur Cell Mater 21 (2011) 130-43.

[111] P. Ducy, T. Schinke, G. Karsenty, The Osteoblast: A Sophisticated Fibroblast under Central Surveillance, Science 289(5484) (2000) 1501-1504.

[112] T. Stigbrand, Present status and future trends of human alkaline phosphatases, Progress in clinical and biological research 166 (1984) 3-14.

[113] N. Datta, Q.P. Pham, U. Sharma, V.I. Sikavitsas, J.A. Jansen, A.G. Mikos, In vitro generated extracellular matrix and fluid shear stress synergistically enhance 3D osteoblastic differentiation, Proceedings of the National Academy of Sciences of the United States of America 103(8) (2006) 2488-93.

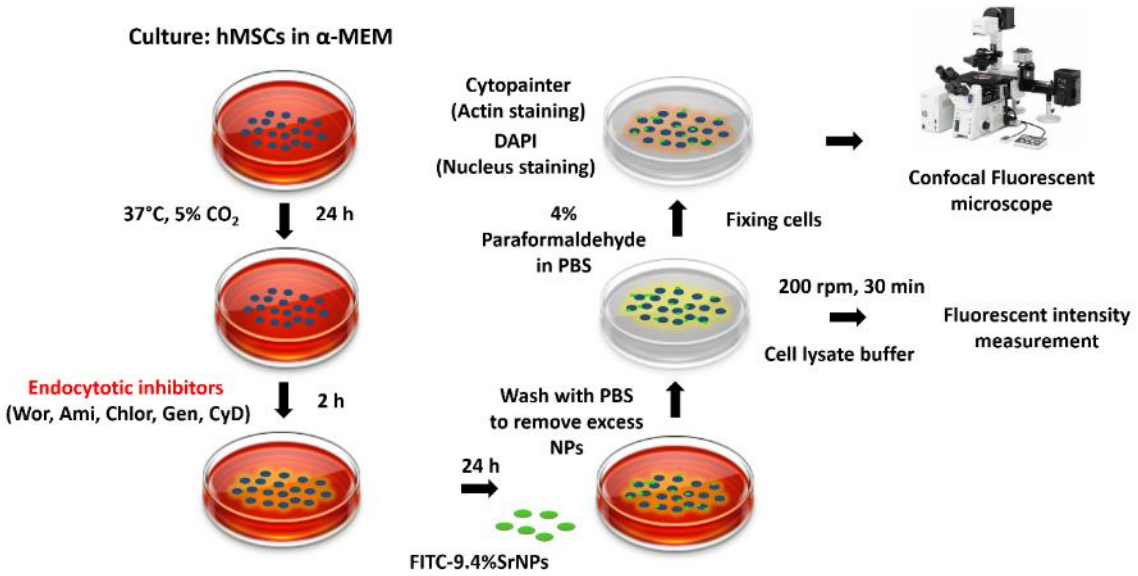
[114] F. Pournaqi, A. Ghiaee, S. Vakilian, A. Ardeshirylajimi, Improved proliferation and osteogenic differentiation of mesenchymal stem cells on polyaniline composited by polyethersulfone nanofibers, Biologicals 45 (2017) 78-84.

[115] M. Lievremont, J. Potus, B. Guillou, Use of alizarin red S for histochemical staining of Ca2+ in the mouse; some parameters of the chemical reaction in vitro, Acta anatomica 114(3) (1982) 268-80.

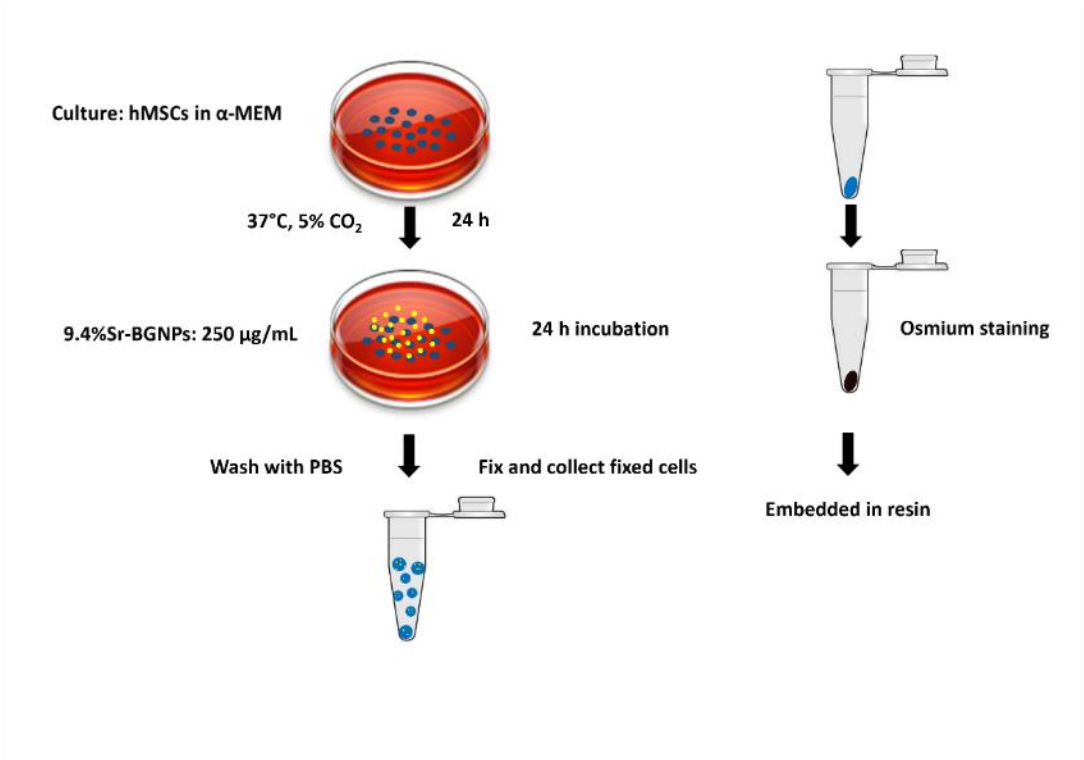
[116] I. Cacciotti, Bivalent cationic ions doped bioactive glasses: the influence of magnesium, zinc, strontium and copper on the physical and biological properties, Journal of Materials Science 52(15) (2017) 8812-8831.

[117] M. Bohner, Resorbable biomaterials as bone graft substitutes, Materials Today 13(1) (2010) 24-30.

Captions



Scheme 1**:** Endocytosis study through the confocal fluorescent microscope and indirect measurement of FITC-9.4**%**Sr-BGNPs endocytosis mechanism**.**



Scheme 2**:** Preparation of biological TEM samples**.**

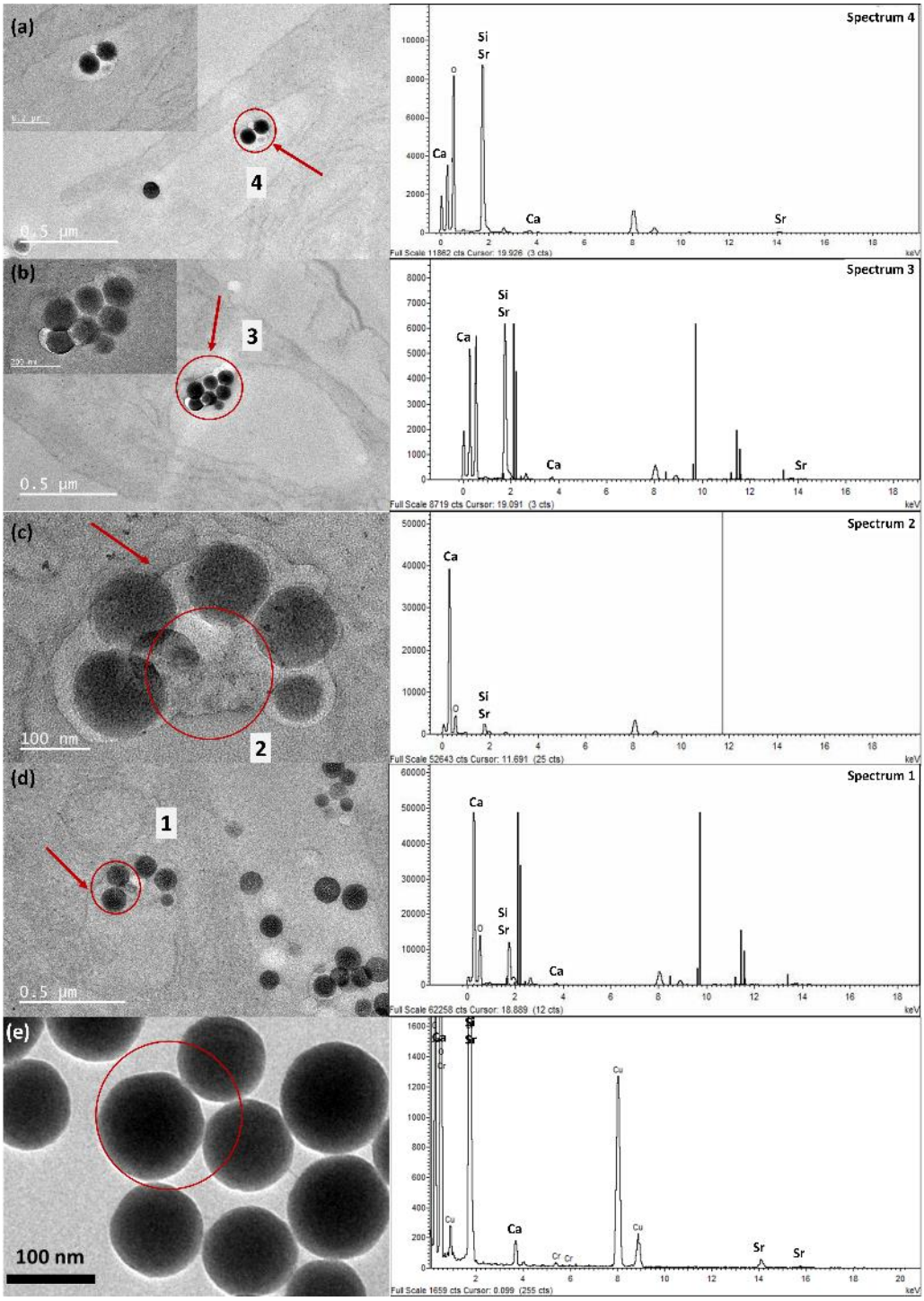


Fig. 1**:** TEM images **(**left panel**)** of monolayer hMSCs exposed to 9.4%Sr-BGNPs at a concentration of 250 µg**/**mL for 24 h incubation **(**a**)** and **(**c**)** show the individual particles inside lysosome vesicles (arrows), **(**b**)** and **(**d**)** show the degraded particles inside these vesicles, and (e) show the unreacted monodispersed particles. EDS spectra **(**right panel**)** represent the elemental components of 9.4%Sr-BGNPs **(**taken from the red circled regions of the corresponding images in the left panel**)**.

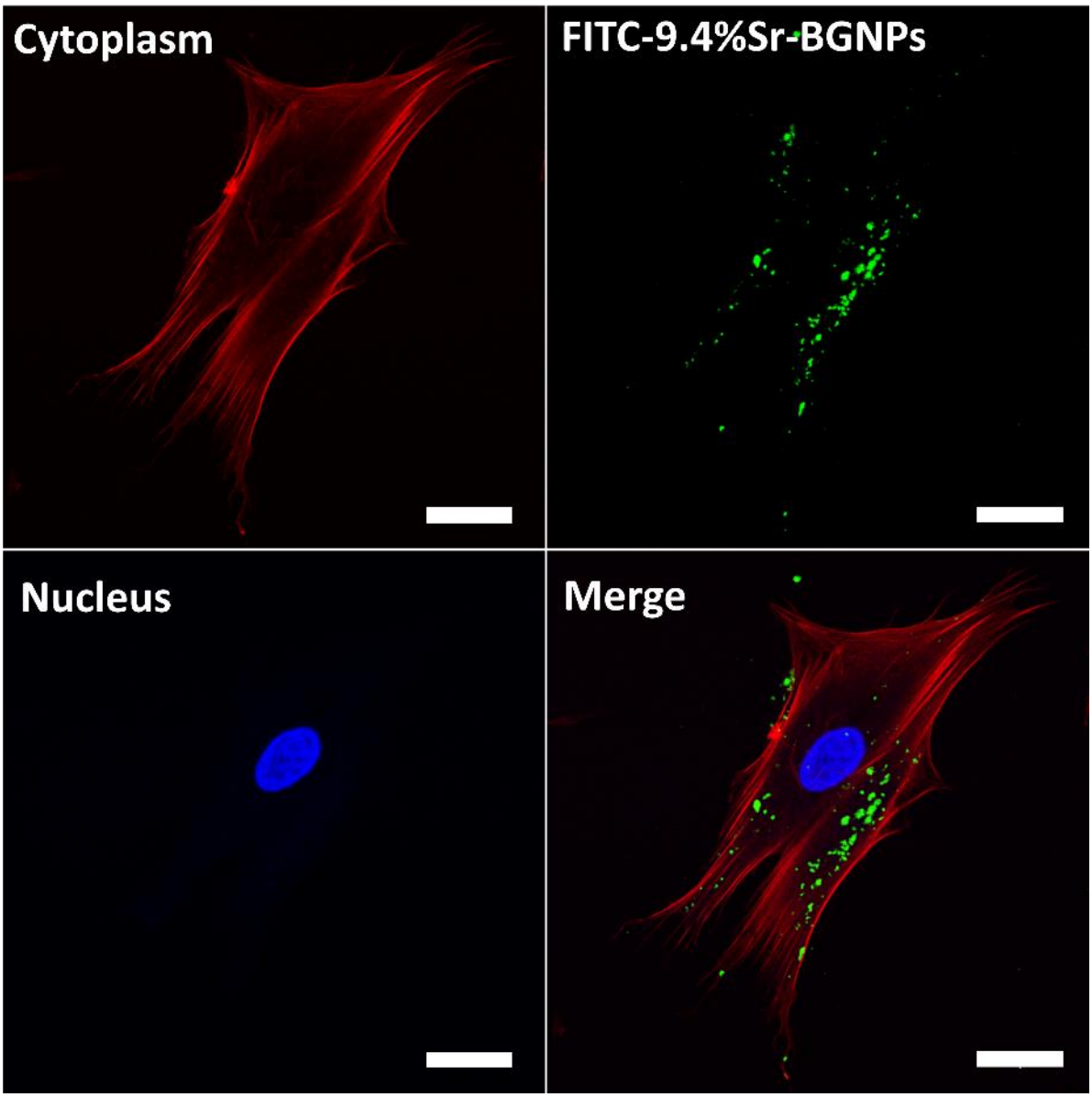


Fig. 2**:** Fluorescent images showing a) the cytoplasm (red), b) the intracellular FITC-9.4%Sr-BGNPs (green) within hMSCs, c) the nucleus (blue) and d) a merge of the 3-channels following 4 h incubation with the particles (Scale bars**:** 25 µm).

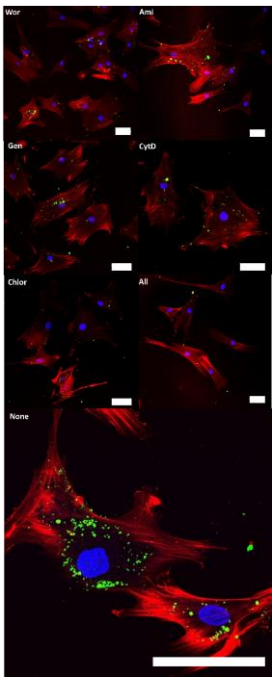


Fig. 3**:** Confocal fluorescence images of the hMSCs **(**red**:** cytoplasm and blue**:** nucleus**)** after 24 h incubation with 250 µg**/**mL FITC**-**9.4%Sr**-**BGNPs in the presence and absence of inhibitor pre-treatment, for the identification of endocytosis mechanisms involved in cellular uptake of FITC**-**9.4%Sr**-**BGNPs by the hMSCs. Pharmacological inhibitors**:** Wor **(**wortmannin**)**, Ami **(**amiloride hydrochloride hydrate**)**, Chlor **(**chlorpromazine**)**, Gen **(**genistein**)**, CytD **(**cytochalasin D**)**. Scale bar is 75 µm**.**

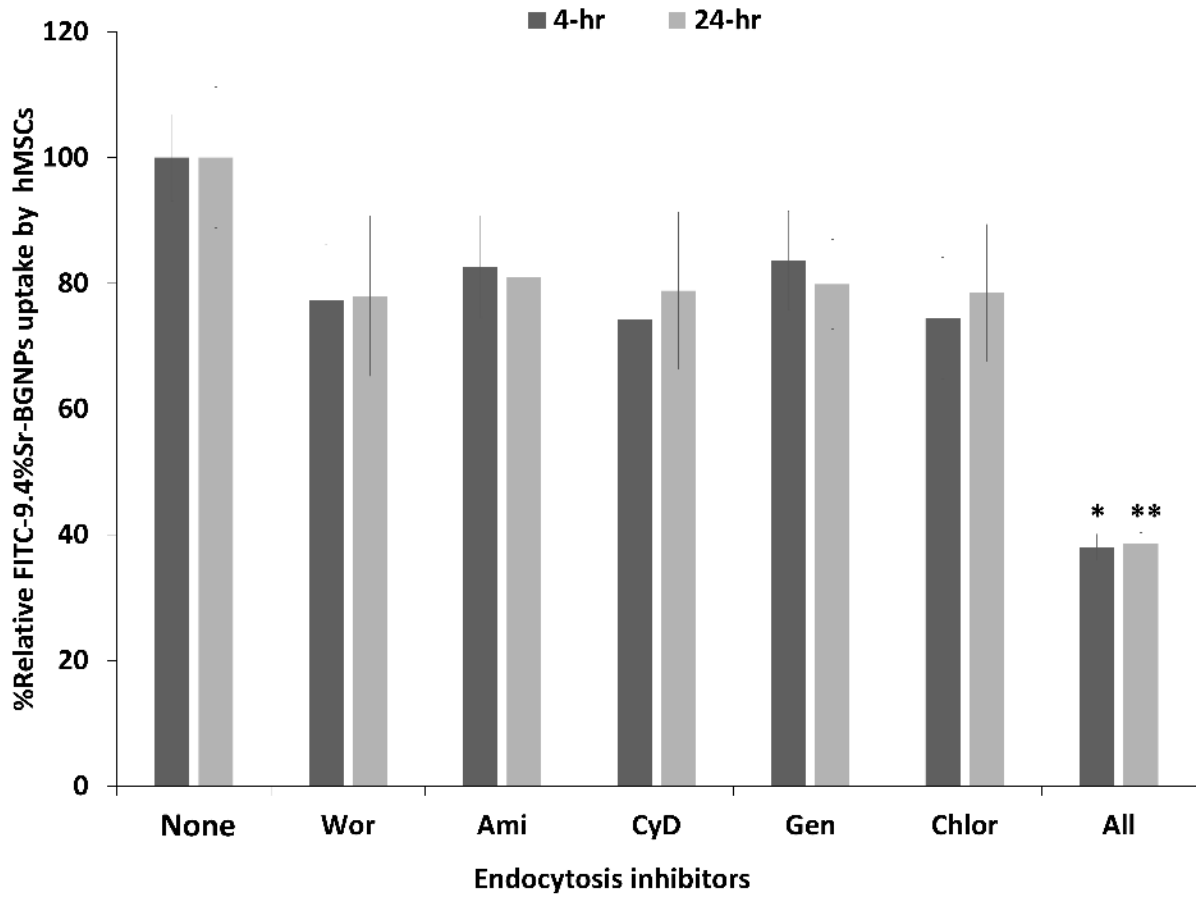


Fig. 4**:** Effect of endocytosis inhibitors on FITC-9.4%Sr-BGNPs **(**concentration at 250 µg**/**mL**)** internalisation by hMSCs after 4 h and 24 h of incubation: Wor **(**wortmannin**)**, Ami **(**amiloride hydrochloride hydrate**)**, Chlor **(**chlorpromazine**)**, Gen **(**genistein**)**, CytD **(**cytochalasin D**).** The values are the mean ± SD of triplicate wells**. ***, ** indicate a statistical difference from the control for 4h (*) and 24h (**), *p<0.05.* The fluorescent intensity of lysed cells was measured and normalised with respect to the positive control (cells cultured in inhibitor-free medium).

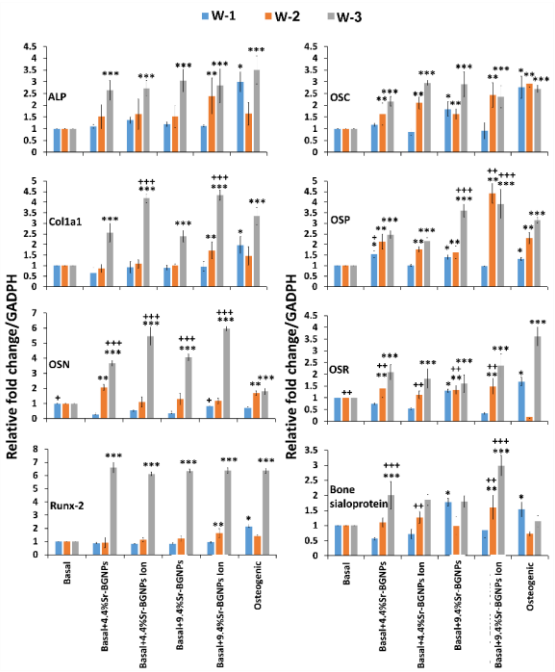


Fig. 5**:** Quantitative real-time reverse transcriptase PCR analysis showing the expression of osteogenic marker genes in hMSCs treated with 4.4**%**Sr-BGNPs, 9.4%Sr-BGNPs, and their dissolution products, cultured under the basal condition for 1, 2 and 3 weeks**.** Gene expression was normalized to GAPDH **(**a housekeeping gene**)** transcript levels**.** The data represent two independent experiments**.** The values are the mean ± SD, n=4**.** The expression of osteogenic marker genes was significantly up-regulated at the indicated times in cells treated with particles and their dissolution products compared to untreated cells**. *** and **+** above the bars represent a significant difference between treated hMSCs versus untreated hMSCs under the basal condition and osteogenic condition respectively**. (***P < 0.05*; *****, **+:** W-1, ******, **++:** W-2 and *******, **+++:** W-3**).**

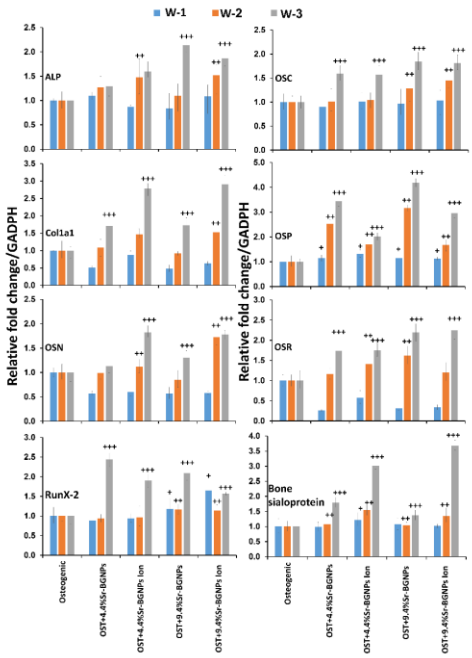


Fig. 6**:** Quantitative real-time reverse transcriptase PCR analysis of the expression of osteogenic marker genes in hMSCs treated with 4.4**%**Sr-BGNPs, 9.4%Sr-BGNPs, and their dissolution products, cultured under the osteogenic condition for 1, 2 and 3 weeks**.** Gene expression was normalized to GAPDH transcript levels**.** The data represent two independent experiments**.** The values are the mean ± SD, n=4**.** The expression of osteogenic marker genes was significantly up-regulated at the indicated times in cells treated with particles and their dissolution products compared to untreated cells **(***P < 0.05*; **+:** W-1, **++:** W-2 and **+++:** W-3**).**

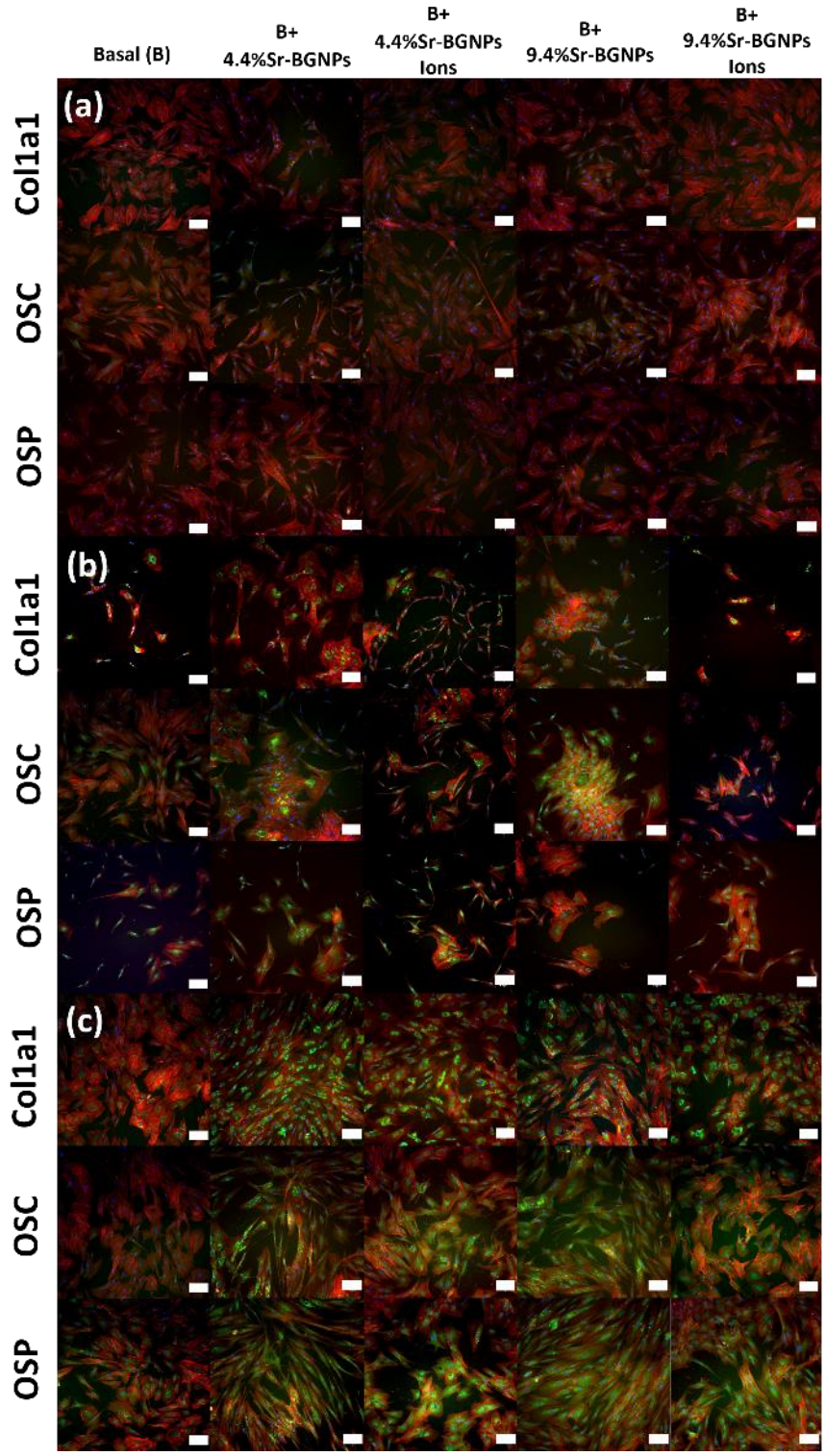


Fig. 7**:** Fluorescence images of hMSCs after 24 h exposure to 9.4**%**Sr-BGNPs and their ion dissolution products **(**Sr-BGNP concentration at 250 µg**/**mL**)**, in the basal condition, followed by a 3-week culture period **(**a**)** W-1, **(**b**)** W-2, and **(**c**)** W-3**:** DAPI **(**blue**)**, **(**a**)** Col1a1, **(**b**)** OSC and **(**c**)** OSP staining **(**all green**)** Scale bar: 150 µm**.**

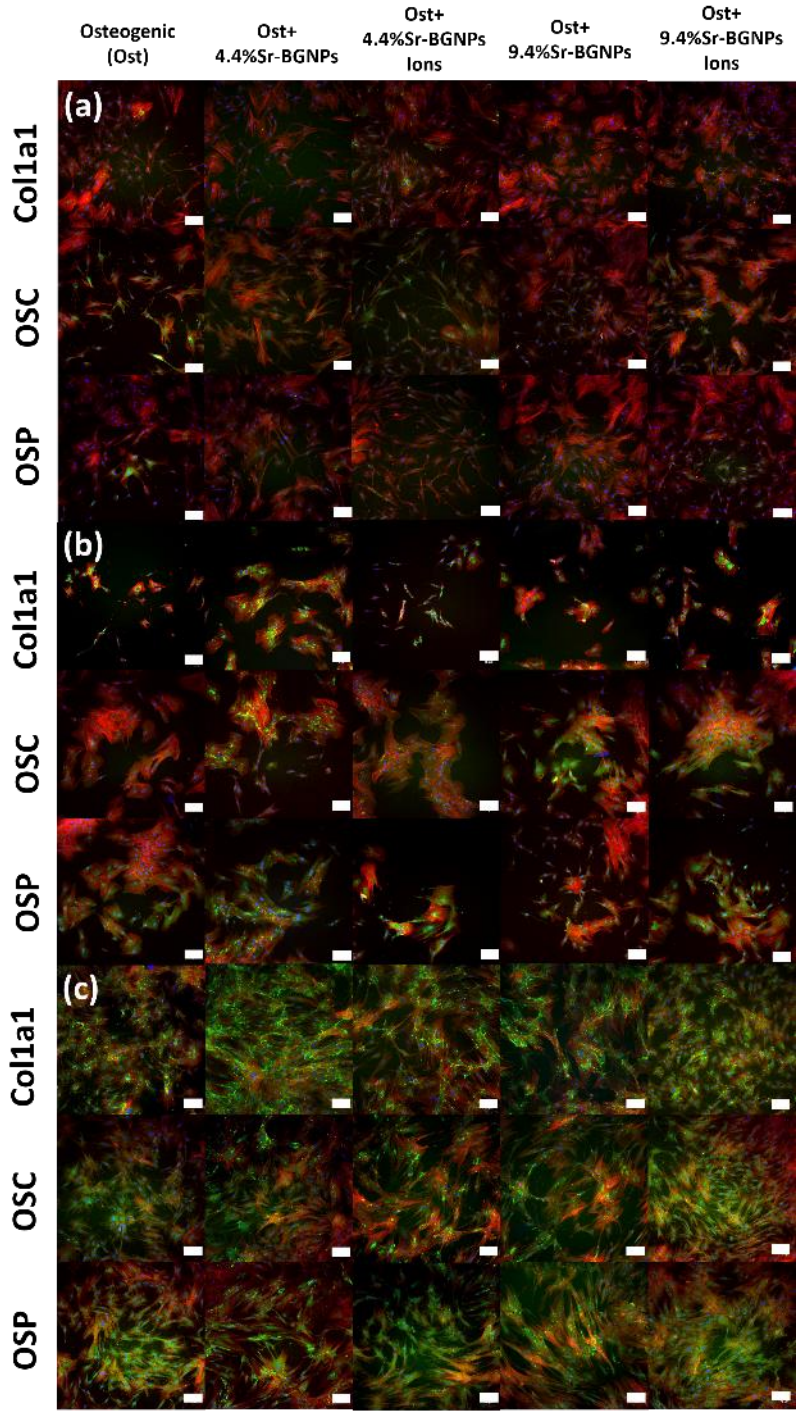


Fig. 8**:** Fluorescence image, DAPI **(**blue**)**, Cytoplasm **(**Red**)**, Col1a1, OSC and OSP staining **(**all green**)** of hMSCs after exposure to 4.4**%**Sr-BGNPs, 9.4**%**Sr-BGNPs or their dissolved ion release products **(**Sr-BGNP concentration at 250 µg**/**mL**)**, in osteogenic condition, followed by a 3-week culture period, **(**a**)** W-1, **(**b**)** W-2, and **(**c**)** W-3**.** Scale bar; 150 µm.

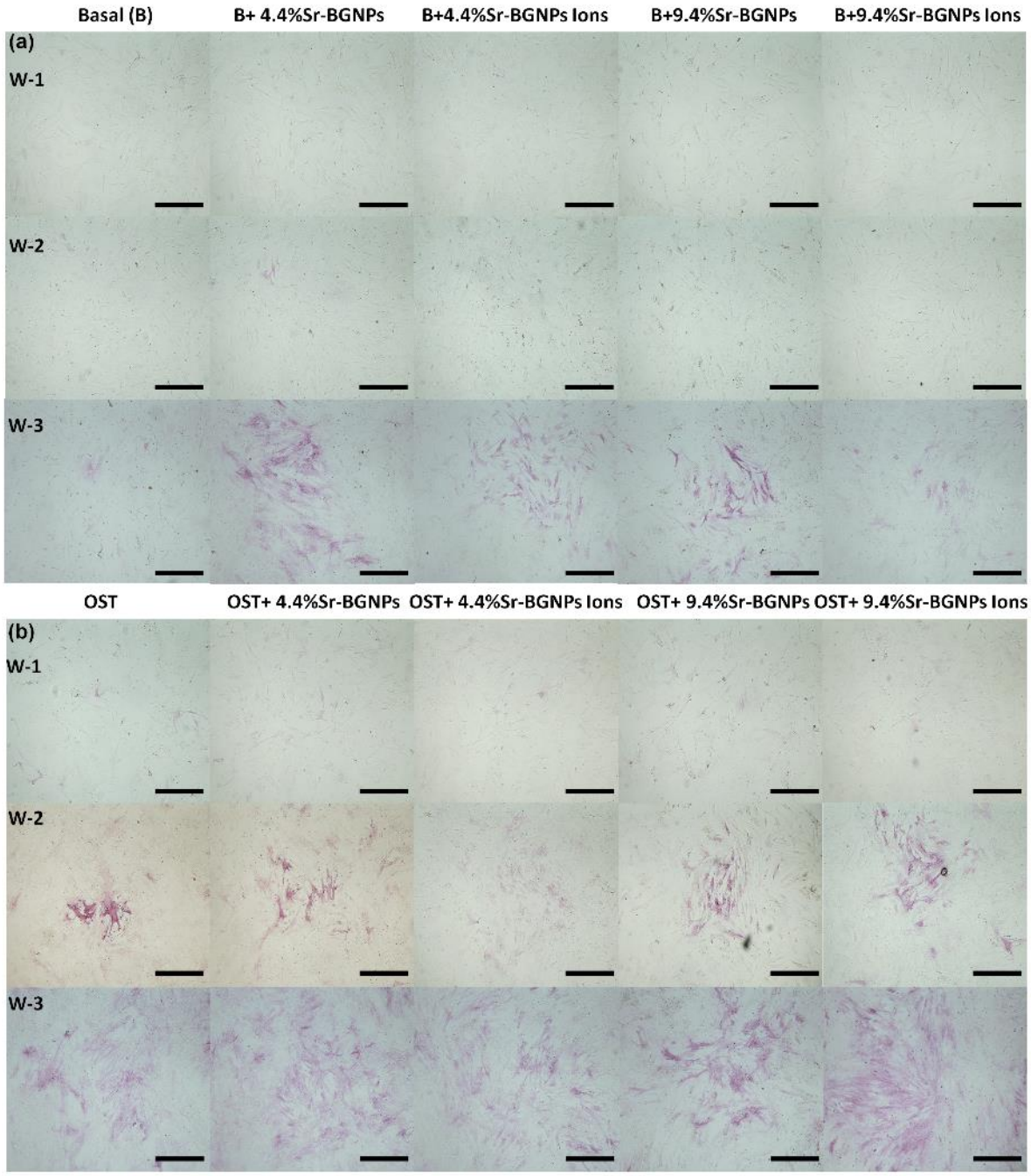


Fig. 9**:** Staining for ALP enzymatic activity of hMSCs cultured in media containing 4.4**%** Sr-BGNPs, 9.4**%** Sr-BGNPs or their dissolution products **(**Sr-BGNP concentration at 250 µg**/**mL**)** for three weeks under **(**a**)** basal and **(**b**)** osteogenic conditions**.** Scale bar; 200 µm.

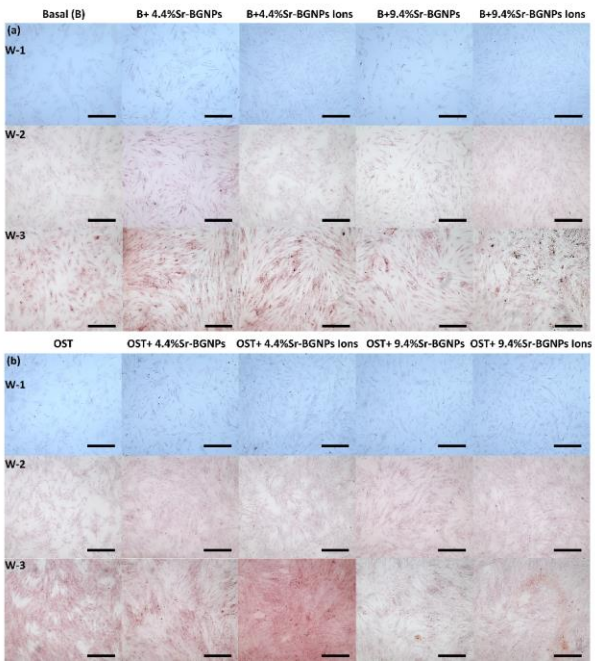


Fig. 10**:** Alizarin red staining of calcified nodules formed by hMSCs treated with 4.4**%** Sr-BGNPs, 9.4**%**Sr-BGNPs or their dissolution ions **(**Sr-BGNP concentration at 250 µg**/**mL**)** for three weeks in culture under **(**a**)** basal and **(**b**)** osteogenic conditions**.** Scale bar; 200 µm.

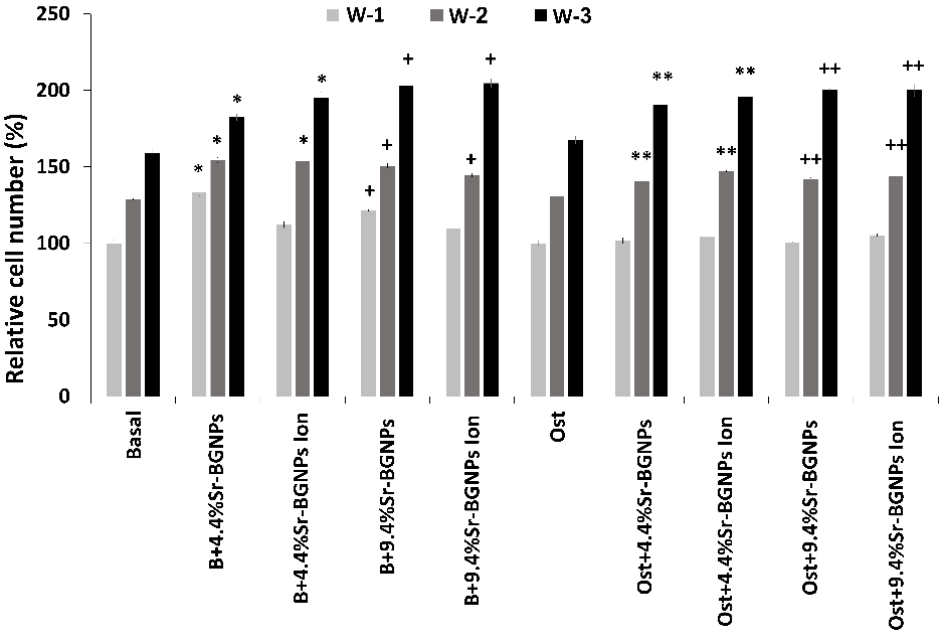


Fig. 11**:** Quantitative analysis of Alizarin red staining to show calcified nodule formation by the hMSCs treated with a 24 h pulse of 4.4**%** Sr-BGNPs and 9.4**%** Sr-BGNPs or the ionic release products **(**Sr-BGNP concentration at 250 µg**/**mL**)** under both the basal and osteogenic conditions**. ***, **** (**4.4**%**Sr-BGNPs**)** and **+**, **++ (**9.4**%**Sr-BGNPs**)** indicate a statistical difference from the control **(*** and **+** for basal, ****** and **++** for osteogenic**)** at the same interval time, *p<0.05***.**

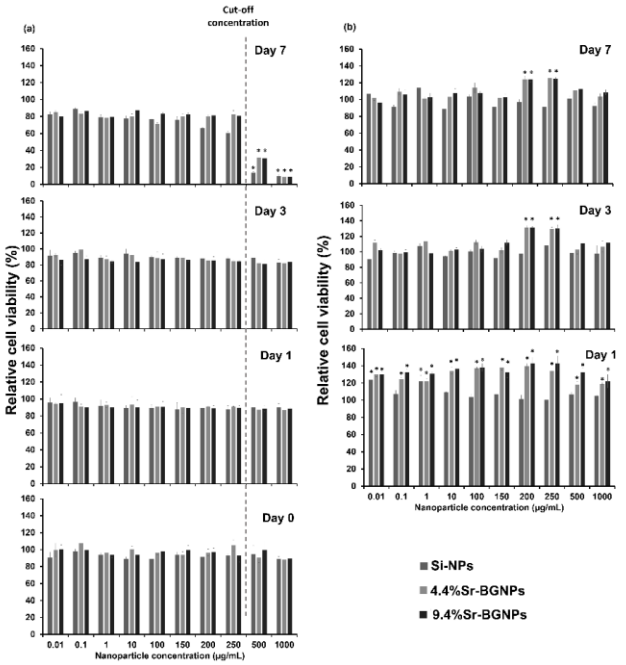


Fig.12**:** Effect of **(**a**)** 4.4%Sr**-**BGNPs and 9.4%Sr-BGNPs and **(**b**)** their dissolution products, on cell viability of hMSCs based on MTT assay after 24 h pulse phase followed by a chase in culture for 0, 1, 3, and 7 days **(**n **=** 6 per group**).** Cells were treated with different concentrations of the particles/ions **(**0**.**01**-**1000 µg**/**mL**). *** indicates a statistical difference from the control, *p<0.05.*

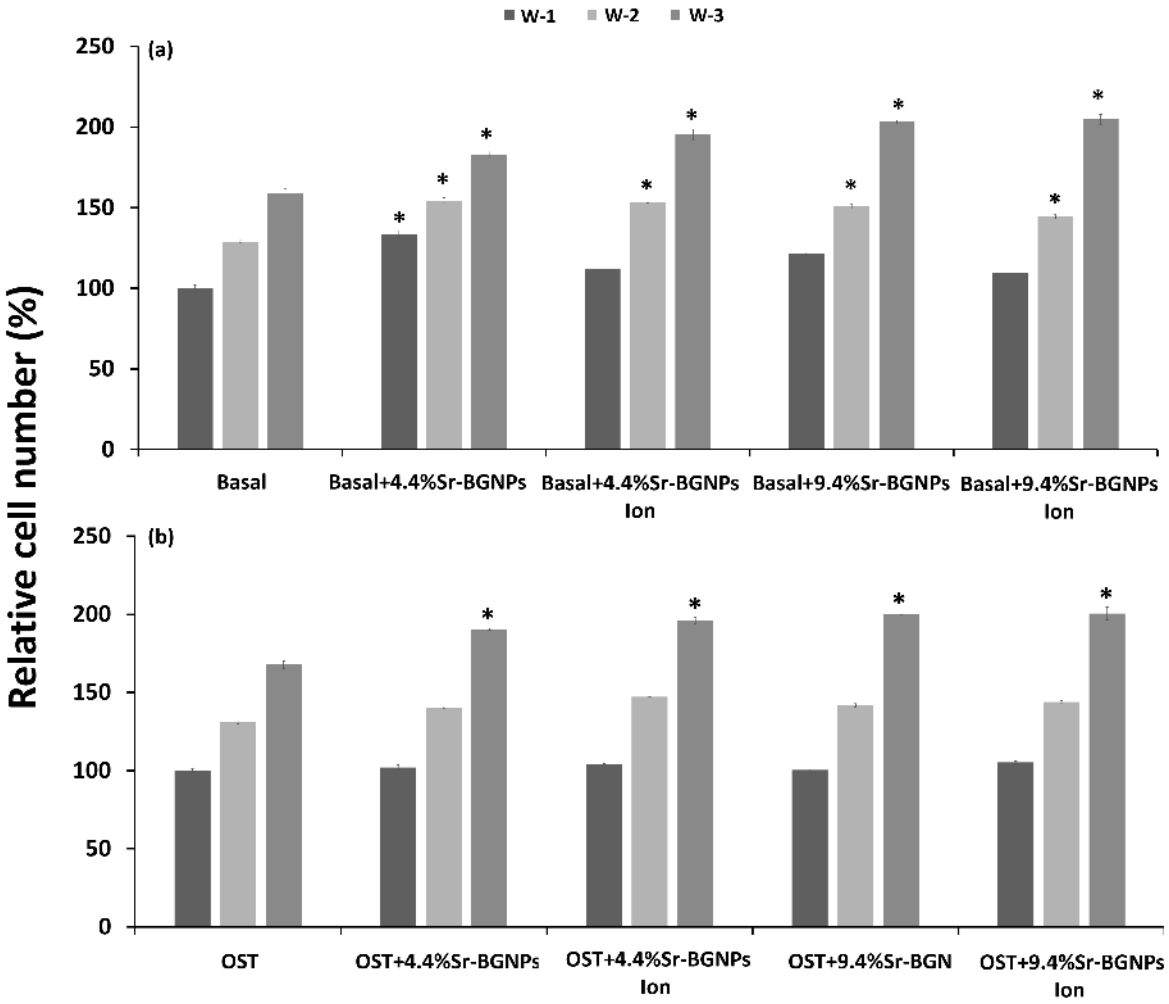
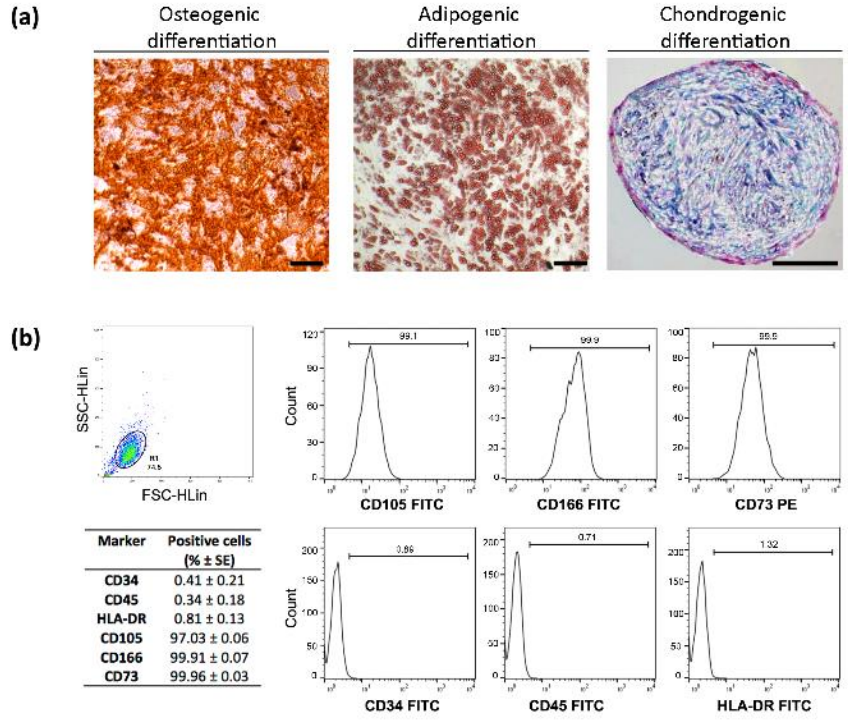


Fig. 13**:** DNA assay of hMSCs after exposure to 4.4**%**Sr-BGNPs, 9.4%Sr-BGNPs or their ionic release product **(**Sr-BGNP concentration at 250 µg**/**mL**)**, using Hoechst 33285 following W-1, W-2 and W-3 in **(**a**)** basal condition and **(**b**)** osteogenic condition**.** *, **+** indicate a statistical difference from the control **(*:** basal and **+:** osteogenic**)** at the same interval time, p<0**.**05**.**

Supplementary videos: The cellular uptake of FITC-9.4%Sr-BGNPs by hMSCs after 24 h incubation with 250 µg/mL FITC-9.4%Sr-BGNPs.



Marker	Positive cells (% ± SE)
CD34	0.41 ± 0.21
CD45	0.34 ± 0.18
HLA-DR	0.81 ± 0.13
CD105	97.03 ± 0.06
CD166	99.91 ± 0.07
CD73	99.96 ± 0.03

Supplementary Figure 1: Differentiation potential of hMSCs and immunophenotypic characterisation. (a) Representative images of alizarin Red S stained calcium deposition after 21 days (osteogenic differentiation), Oil Red O stained neutral lipids in the cytoplasm after 14 days (adipogenic differentiation) and secretion of Alcian Blue stained sulfated proteoglycans (chondrogenic differentiation); (b) representative histograms of expression of hMSC cell surface markers: untreated hMSCs in suspension at P2 were labelled with FITC or PE-conjugated monoclonal antibodies for CD105, CD166, CD73, CD34, CD45 and HLA-DR. The cell size of subpopulations with the selected (gated) population is also shown, SSC = side scattered light, FSC = forward scattered light along with the percentage (%) of positive cells ± standard error (SE) of the analyzed surface markers.

Table 1: Elemental compositions of 4.4%Sr-BGNPs, 9.4% Sr-BGNPs and dense silica controls (Si-NPs) after thermal processing and washing, measured by ICP of solutions following lithium metaborate fusion.

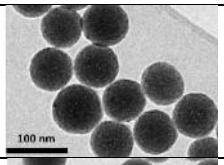
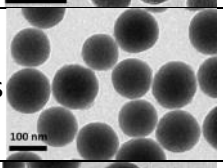
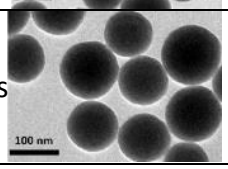
Samples	% mol.		
	Si	Ca	Sr
Si-NPs 	100.0±0.0	0±0.0	0±0.0
4.4%Sr-BGNPs 	90.6±0.2	5.0±0.1	4.4±0.0
9.4%Sr-BGNPs 	88.8±0.3	1.8±0.2	9.4±0.0

Table 2**:** Primers used for real time RT-PCR**.**

Gene	**Primer sequences**	**Amplicon size**
Human Runx-2 (*runx-2*) *(NM_001024630, NM_001015051)*	F: 5’ gta gat gga cct cgg gaa cc 3’ R: 5’ gag gcg gtc aga gaa caa ac 3’	78 bp
Human Osterix (*osr*) *(NM_152860)*	F: 5’ atg ggc tcc ttt cac ctg 3’ R: 5’ ggg aaa agg gag ggt aat c 3’	75 bp
Human ALP (*alp*) *(NM_000478)*	F: 5’ gga act cct gac cct tga cc 3’ R: 5’ tcc tgt tca gct cgt act gc 3’	86 bp
Human Col1a1 (*col1a1*) *(NM_ 000088)*	F: 5’ gag tgc tgt ccc gtc tgc 3’ R: 5’ ttt ctt ggt cgg tgg gtg 3’	52 bp
Human Bone Sialoprotein (NM_004967)	F: 5’ cag ttc aga aga gga gg 3’ R: 5’ tca gcc tca gag tct tca tc 3’	100 bp
Human Osteonectin (*osn*) *(NM_003118)*	F: 5’ gag gaa acc gaa gag gag g 3’ R: 5’ ggg gtg ttg ttc tca tcc ag 3’	95 bp
Human Osteopontin (*osp*) *(NM_001040058, NM_000582, NM_001040060)*	F: 5’ gtt tcg cag acc tga cat cc 3’ R: 5’ cat tca act cct cgc ttt cc 3’	80 bp
Human Osteocalcin (*osc*) *(NM_199173)*	F: 5’ ggc agc gag gta gtg aag ag 3’ R: 5’ ctc aca cac ctc cct cct g 3’	102 bp

Table 3. Elemental concentration of Si, Ca and Sr in the media of dissolution products from the bioactive glass nanoparticles in α-MEM.

NPs	**[Si] (μg/mL)**	**[Ca] (μg/mL)**	**[Sr] (μg/mL)**
4.4%Sr-BGNPs	27.2	6.0	3.0
9.4%Sr-BGNPs	28.1	2.1	6.3